

Chiral Donor Photoinduced-Electron-Transfer (d-PET) Boronic Acid Chemosensors for the Selective Recognition of Tartaric Acids, Disaccharides, and Ginsenosides

Yubo Wu,^[a] Huimin Guo,^[a] Xin Zhang,^[a] Tony D. James,^[b] and Jianzhang Zhao*^[a]

Abstract: A modular approach was proposed for the preparation of chiral fluorescent molecular sensors, in which the fluorophore, scaffold, and chirogenic center can be connected by ethynyl groups, and these modules can easily be changed to other structures to optimize the molecular sensing performance of the sensors. This modular strategy to assembly chiral sensors alleviated the previous restrictions of chiral boronic acid sensors, for which the chirogenic center, fluorophore, and scaffold were integrated, thus it was difficult to optimize the molecular structures by chemical modifications. We demonstrated the potential of our new strategy by the preparation of a sensor with a larger scaffold. The photo-

induced electron-transfer (PET) effect is efficient even with a large distance between the N atom and the fluorophore core. Furthermore, the rarely reported donor-PET (d-PET) effect, which was previously limited to carbazole, was extended to phenothiazine fluorophore. The contrast ratio, that is, PET efficiency of the new d-PET sensor, is increased to 8.0, compared to 2.0 with the previous carbazole d-PET sensors. Furthermore, the ethynylated phenothiazine shows longer excitation wavelength (centered at 380 nm) and emission wavelength (492 nm), a large

Keywords: boronic acids • chirality • fluorescence • ginsenosides • sensors

Stokes shift (142 nm), and high fluorescence quantum yield in aqueous solution ($\Phi = 0.48$ in MeOH/water, 3:1 v/v). Enantioselective recognition of tartaric acid was achieved with the new d-PET boronic acid sensors. The enantioselectivity is up to 10 (ratio of the binding constants toward D- and L-tartaric acid, k_D/k_L). A consecutive fluorescence enhancement/decrease was observed, thus we propose a transition of the binding stoichiometry from 1:1 to 1:2 as the analyte concentration increases, which is supported by mass spectra analysis. The boronic acid sensors were used for selective and sensitive recognition of disaccharides and glycosylated steroids (ginsenosides).

Introduction

Chiral fluorescent chemosensors are important for the detection of chiral analytes.^[1–9] Fluorescent chiral boronic acid sensors are of particular interest due to the covalent bonding nature of the enantioselective interaction between the sensor and the analytes (such as tartaric acids, sugar, sugar alcohol, and sugar acids), which ensures their applicability for the analysis of biological samples.^[10–26]

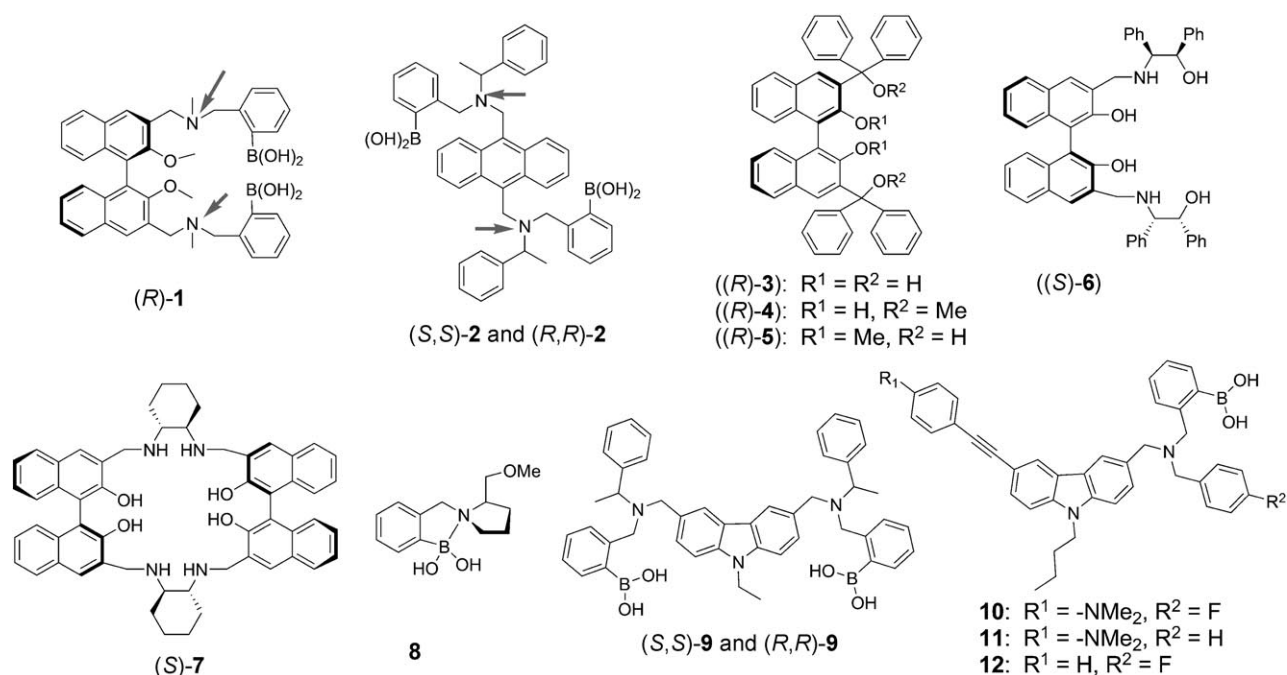
We have long been interested in chiral fluorescent boronic acid sensors.^[25] Previously, a chiral boronic acid sensor for the recognition of glucose was reported (Scheme 1, sensor

1).^[26] For **1**, the 1,1'-bi-2-naphthol (BINOL) moiety plays the role of fluorophore, scaffold, and the chirogenic center as well. In a later study we used the same BINOL-based chiral boronic acid sensors for enantioselective recognition of tartaric acids.^[25a] However, the BINOL fluorophore emits UV light, whereas emission in the visible region is desired. Furthermore, the fluorophore and the chirogenic centers of the BINOL-based chiral sensors are integrated (the same is true for the chiral sensors **1–7** and sensor **9**, Scheme 1),^[2,25a,b,f,g,26–29] thus it is difficult to change the fluorophores, scaffold, or the binding sites to other structures to optimize the molecular sensing performance, such as the emission and recognition properties of the sensors.^[25a] To tackle these limitations to some extent, we developed anthracene-based chiral boronic acid sensors, which demonstrated visible emission and good chiral selectivity toward tartaric acid, sugar acids, and sugar alcohols (sensor **2**, Scheme 1).^[25b–d] More recently, we devised carbazole-based donor photoinduced-electron-transfer (d-PET) chiral boronic acids **9** and **10**, with the fluorophore as the electron donor of the photoinduced electron transfer (d-PET), and a protonated amine/boronic acid moiety as the acceptor of the PET (a-PET); the background emission for the sensor at acidic pH is much lower than with normal a-PET sensors.^[25e,f] However, the carbazole fluorophores in these sensors

[a] Y. Wu, Dr. H. Guo, X. Zhang, Prof. J. Zhao
State Key Laboratory of Fine Chemicals
School of Chemical Engineering
Dalian University of Technology
Dalian 116024 (P.R. China)
Fax: (+86) 411-8498-6236
E-mail: zhaojzh@dlut.edu.cn

[b] Dr. T. D. James
Department of Chemistry, University of Bath
Bath, BA2 7AY (UK)

Supporting information for this article is available on the WWW under <http://dx.doi.org/10.1002/chem.201100033>.



Scheme 1. Typical chiral fluorescence molecular sensors (**1–9**) with integrated fluorophore, molecular scaffold, and chirogenic centers. (Sensors **10–12** are not chiral. The structures are presented for comparison). The N atoms that serve as the fluorescence switch in some typical PET sensors are marked by arrows in sensors **1** and **2**.

also serve as the scaffold, therefore this is still an integrated molecular sensor.

The drawbacks of the current chiral boronic acid sensors are as follows. 1) The fluorophore, scaffold, and the chirogenic centers are integrated (sensor **1**, **3–7**, Scheme 1). Thus the selection of the fluorophore for chiral sensors is limited to those with the dialdehyde motif. Because the chiral boronic acid sensors usually require two binding sites, a dialdehyde motif is necessary to access the chiral boronic acid sensors. 2) The typical fluorophore used for boronic acid sensors are anthracene, BINOL, or naphthalene. The emission wavelength of these chiral boronic acid sensors are usually at near-UV region. A tailored fluorophore cannot be used due to the intrinsic drawbacks of the structural motif mentioned in the first point. 3) Currently, the fluorophores of the d-PET boronic acid sensors are restricted to carbazole, which gives off UV emissions.^[25f–k] 4) The PET efficiency of the d-PET boronic acid sensors that use carbazole as the fluorophore is low; the emission enhancement (or the contrast ratio) is approximately twofold upon switching the pH from acidic pH to neutral pH. The a-PET sensor **2** (Scheme 1) displays a contrast ratio of 10.^[25b]

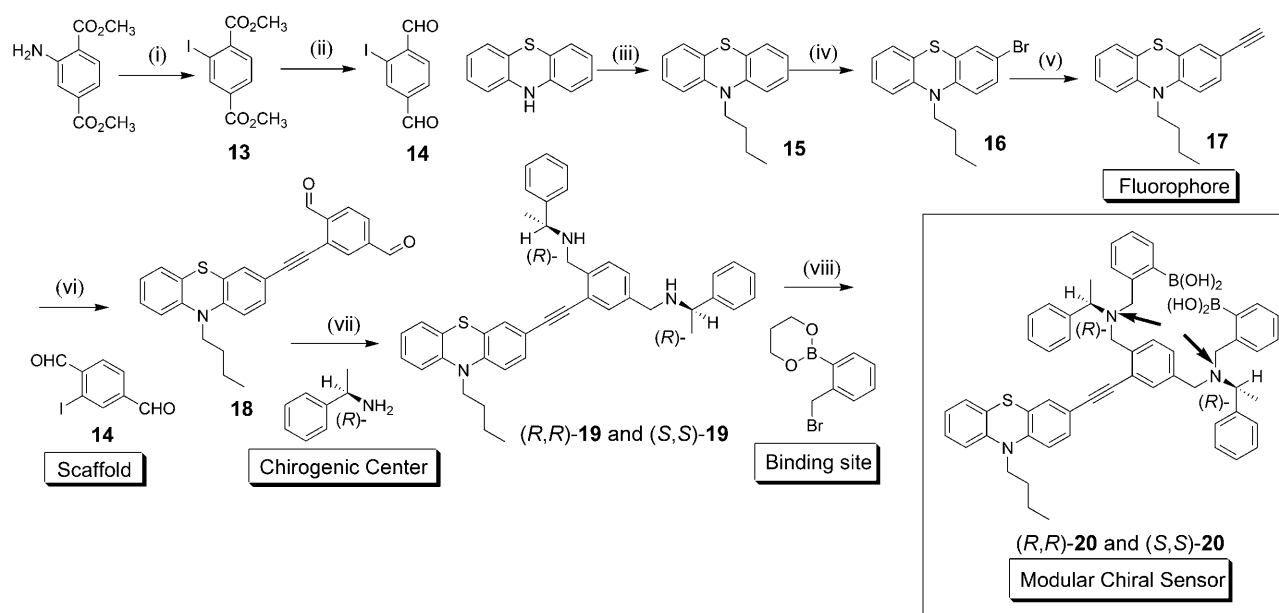
To tackle the aforementioned limitations, herein we propose a modular approach to the preparation of chiral boronic acid sensors. With this new strategy to assemble chiral fluorescent sensors, the above challenges were addressed. The sensors were used for enantioselective recognition of disaccharides such as sucrose, lactose, and maltose. We also used the sensors for recognition of glycosylated steroids (ginsenosides). Our modular concept for the construction of a chiral sensor will be useful in the design of new chiral fluorescent

chemosensors with improved enantioselectivity and photo-physical properties.

Results and Discussion

Design and synthesis: We devised sensor **20** (Scheme 2), in which the fluorophore (phenothiazine) and the chirogenic centers ((R) - or (S) - α -benzylamine) were modules and readily assembled onto a scaffold of 2-iodo-1,4-benzenedicarboxaldehyde. The two parts are connected by π conjugation through an ethynylene group ($C\equiv C$). A large distance between the PET switch, that is, the N atom, and the fluorophore core could be potentially detrimental to the PET efficiency (contrast ratio). The ethynylene linker was used instead of ethylene ($C=C$), because it is known that the *cis/trans* isomerization of the $C=C$ double bonds serves as an efficient drainpipe for the excited-state energy, thus the fluorescence could be quenched. For the rigid ethynylene linker, however, efficient through-bond electron/energy transfer can be established. Furthermore, with a rigid linker between the fluorophore and the boronic acid binding sites, the interaction between the binding sites and the fluorophore can be avoided.^[25d] We selected phenothiazine as the fluorophore for the d-PET effect because of its well-known strong electron-donating ability.^[30,31] Thus we expected that the contrast ratio of the d-PET effect of the new sensors may be improved relative to our previously reported carbazole-based d-PET fluorescent boronic acid sensors.^[25f–h]

The binding pocket of sensor **20** is similar to the anthracene-based chiral boronic acid sensors reported by us previ-



Scheme 2. Synthesis of the chiral fluorescent boronic acid sensor **20** by using a modular approach. Reagents and conditions: i) NaNO_2 , HCl , 0°C , 45 min, KI , 18 h, RT, 26%; ii) $\text{AlH}(\text{iBu})_2$, $\text{THF}/\text{hexane}(1:1)$, -78°C , 6 h, NH_4Cl ; pyridinium chlorochromate, CH_2Cl_2 , 24 h, 30%; iii) phenothiazine, hexadecyltrimethylammonium bromide, NaOH , $n\text{C}_4\text{H}_9\text{Br}$, acetone, reflux, 6 h, 60%; iv) bromine, glacial acetic acid, 0°C , 1 h, 70%; v) $[\text{Pd}(\text{PPh}_3)_2\text{Cl}_2]$, CuI , NEt_3 , PPh_3 , ethynyltrimethylsilane argon atmosphere, reflux, 6 h, then K_2CO_3 , MeOH , 1 h, 84%; vi) $[\text{Pd}(\text{PPh}_3)_2\text{Cl}_2]$, CuI , NEt_3 , PPh_3 , nitrogen atmosphere, reflux, 8 h, 40%; vii) (*R*)- and (*S*)- α -methylbenzylamine, THF , reflux, 8 h, then $\text{NaBH}_3(\text{CN})$, 0°C , 30 min, 40% (*S,S*)-**19**, 36% (*R,R*)-**19**; viii) acetonitrile, K_2CO_3 , 2-(2-bromomethylphenyl)-1,3,2-dioxaborinane, reflux, 10 h, 28% (*S,S*)-**20**, 30% (*R,R*)-**20**. The N atoms that serve as the fluorescence switch centers are marked by arrows in sensor **20**.

ously (sensor **2**, Scheme 1).^[25b–d] It should be pointed out that with the modular structural motif of **20**, any fluorophores that can be ethynylated are suitable for attachment to the chirogenic moiety to assemble a chiral sensor and achieve different emission properties, such as wavelength or Stokes shift, and so forth. We will also need to study the PET efficiency or the contrast ratio of the sensors (the variation of the fluorescence emission enhancement with the switching off of the PET quenching effect), because the distance between the N switch and the fluorophore core is quite large.

The synthesis was carried out with phenothiazine as the starting material. Alkylation at the N position and bromination with Br_2 led to **16** and the ethynylated phenothiazine **17** (the fluorophore). Sonogashira coupling with 2-iodo-1,4-benzenedicarboxaldehyde (the modular scaffold) leads to dialdehyde **18**. Then modular chiral sensor **20** ((*R,R*)-**20** and (*S,S*)-**20**) was obtained by reductive amination with chiral amine (α -benzylamine) and finally introduction of the boronic acid subunits (binding sites) to the sensor. Compounds were obtained in moderate to low yields.

To investigate the effect of the size of the binding pocket of the boronic acid sensor on the enantioselective recognition, sensor **25** ((*S,S*)-**25** and (*R,R*)-**25**) was also devised (Scheme 2). The binding pocket of sensor **25** has been extended by using a larger scaffold (Scheme 3). The distance between the PET switch (the N atom) and the fluorophore of **25** is increased further relative to **20**. Thus it will be interesting to investigate the effect of this increased distance on

the contrast ratio of the PET effect of **25**. The analytes are summarized in Scheme 4.

Enantioselective recognition of D- and L-tartaric acid with modular chiral d-PET fluorescent boronic acid sensor **20**:

The emission properties of (*S,S*)-**20** and (*S,S*)-**25** were investigated (Figure 1). With excitation at 375 nm, emission centered at 488 nm was observed ($\Phi=0.487$ in methanol/water, 3:1 v/v). The Stokes shift is up to 138 nm. A slightly redshifted emission at 500 nm was observed for (*S,S*)-**25**. A similar quantum yield was observed for (*S,S*)-**25** ($\Phi=0.310$ in methanol/water, 3:1 v/v). It should be pointed out that the emission maximum ($\lambda_{\text{em}}=492$ nm) is significantly redshifted when compared to the anthracene-based boronic acid sensors ($\lambda_{\text{em}}=429$ nm) or the carbazole-based boronic acid sen-

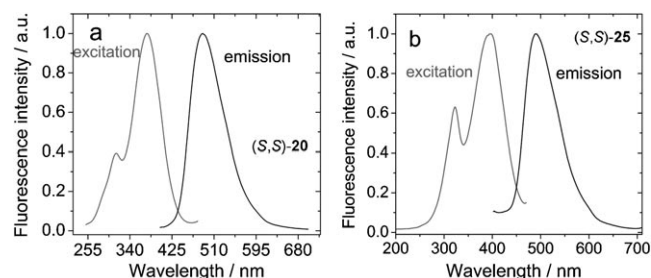
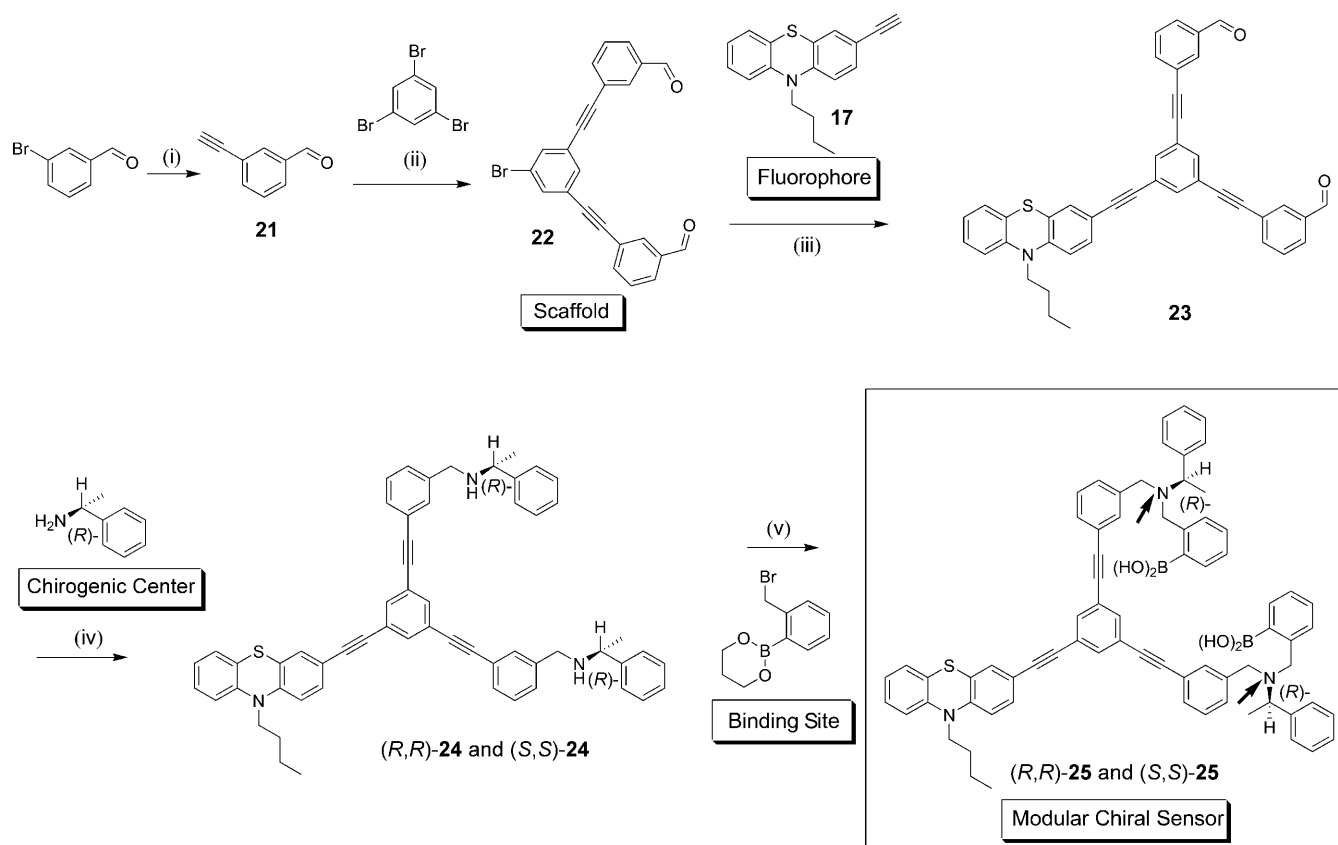


Figure 1. Normalized excitation and emission spectra of (*S,S*)-**20** and (*S,S*)-**25**: a) (*S,S*)-**20**, $\lambda_{\text{ex}}=375$ nm, $\lambda_{\text{em}}=488$ nm; b) (*S,S*)-**25**, $\lambda_{\text{ex}}=380$ nm, $\lambda_{\text{em}}=492$ nm. We used 5.0×10^{-7} mol dm^{-3} of sensors in methanol/water mixed solvent (3:1 v/v), pH 7.0, 20°C .



Scheme 3. Synthesis of the chiral fluorescent boronic acid sensor **25** by using a modular approach. Reagents and conditions: i) $[\text{Pd}(\text{PPh}_3)_2\text{Cl}_2]$, CuI, NEt_3 , ethynyltrimethylsilane, argon atmosphere, reflux, 6 h, then K_2CO_3 , MeOH, 1 h, 81%; ii) $[\text{Pd}(\text{PPh}_3)_2\text{Cl}_2]$, CuI, NEt_3 , 1,3,5-tribromobenzene, argon atmosphere, reflux, 10 h, 60%; iii) $[\text{Pd}(\text{PPh}_3)_2\text{Cl}_2]$, CuI, NEt_3 , PPh_3 , nitrogen atmosphere, reflux, 8 h, 60%; iv) (*R*)- and (*S*)- α -methylbenzylamine, THF, reflux, 8 h, then $\text{NaBH}_3(\text{CN})$, 0°C , 30 min, 75% ((*S,S*)-**24**), 65% ((*R,R*)-**24**); v) acetonitrile, K_2CO_3 , 2-(2-bromomethylphenyl)-1,3,2-dioxaborinane, reflux, 10 h, yields: 32% ((*S,S*)-**25**), 30% ((*R,R*)-**25**). The N atoms that serve as the fluorescence switch centers are marked by arrows in sensor **25**.

sors ($\lambda_{\text{em}} = 375 \text{ nm}$). Furthermore, the larger Stokes shift of sensor **20** (138 nm) relative to the previously reported anthracene-based boronic acid sensor ($\approx 20 \text{ nm}$) and the carbazole-based sensor ($\approx 40 \text{ nm}$) is also beneficial for fluorescence analysis. All these features are ideal for the application of phenothiazine as a novel fluorophore for fluorescent molecular sensors.

The solvent-polarity dependence of the emission of the sensor was investigated (see the Supporting Information). Sensor **20** shows similar emission wavelength and intensity in dichloromethane, methanol, and methanol/water (3:1 v/v). However, sensor **25** shows solvent-polarity-dependent emission (see the Supporting Information). Many fluorophores display solvent-dependent emission, such as Rhodamines, dansylamine, naphthalimide, and so on. Polarity-sensitive emission will complicate fluorescence sensing because the response of the molecular sensors will be dependent not only on the analytes, but also the polarity of the environment. Therefore, fluorophores with polarity-independent emission are desired. Recently, some fluorophores with polarity-independent emission have been tested, such as 4,4-difluoro-4-bora-3a,4a-diaza-*s*-indacene (BODIPY). However,

BODIPY dyes show small Stokes shift (typical Stokes shift is less than 20 nm).

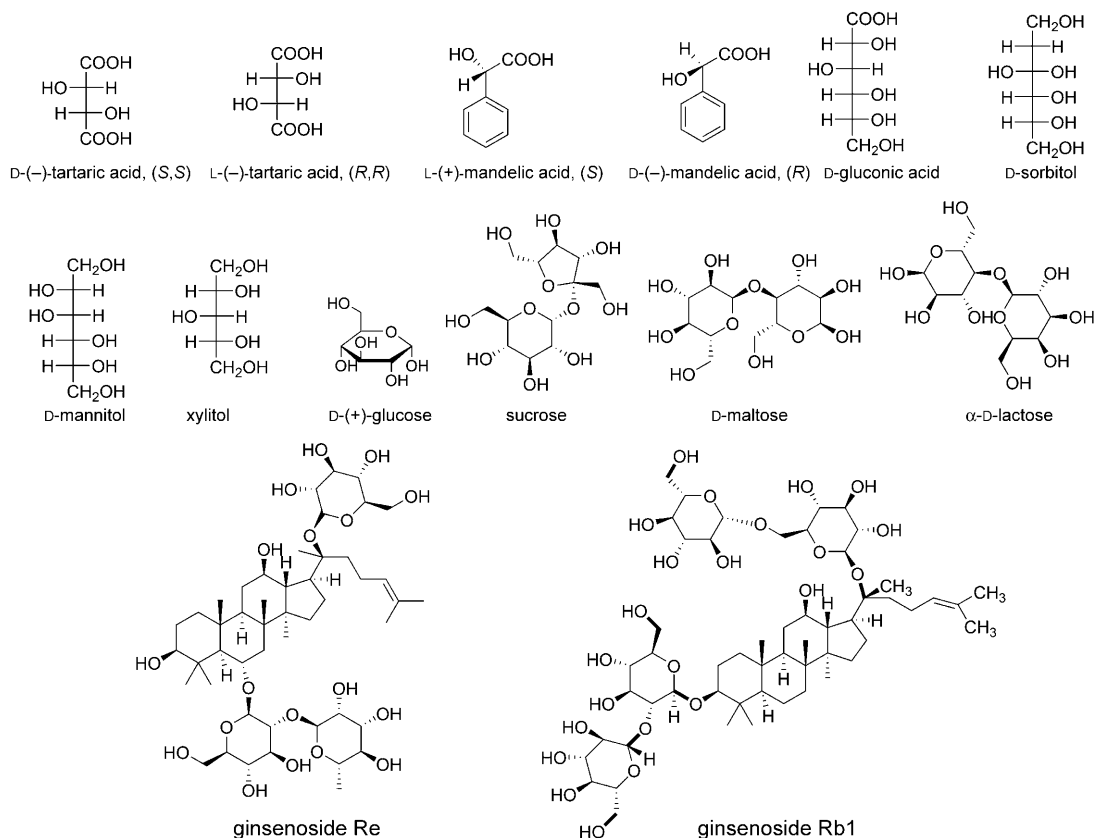
The photophysical parameters are summarized in Table 1. We propose that phenothiazine is a promising fluorophore for the design of molecular chemosensors.

Table 1. Photophysical parameters of sensors **20** and **25**.

Sensors	$\epsilon^{[a]}$	λ_{abs} [nm]	λ_{em} [nm]	Stokes shift [nm]	$\Phi^{[b]}$ pH 3.0	$\Phi^{[b]}$ pH 7.0
(<i>R,R</i>)- 20	1.48×10^4	350	488	138	0.152	0.476
(<i>S,S</i>)- 20	1.43×10^4	350	488	138	0.155	0.487
(<i>R,R</i>)- 25	2.17×10^4	350	492	142	0.033	0.302
(<i>S,S</i>)- 25	2.15×10^4	350	492	142	0.036	0.310

[a] In methanol/water mixed solvent (3:1 v/v), pH 7.0. [b] Fluorescence quantum yields, with quinine sulfate as the standard ($\Phi = 0.54$ in $0.05 \text{ M H}_2\text{SO}_4$). Concentrations of the sensors are $1.0 \times 10^{-5} \text{ mol dm}^{-3}$.

Next, the pH dependence of the emission of sensor **20** was investigated (Figure 2). The sensor displays a weak emission in the acidic pH region but intensified emission in the neutral and the basic pH regions. Thus a d-PET effect



Scheme 4. The chiral analytes used in the study.

(fluorophore as the electron donor of the PET) was observed for sensor **20**.^[25f,h] For the normal a-PET sensors (flu-

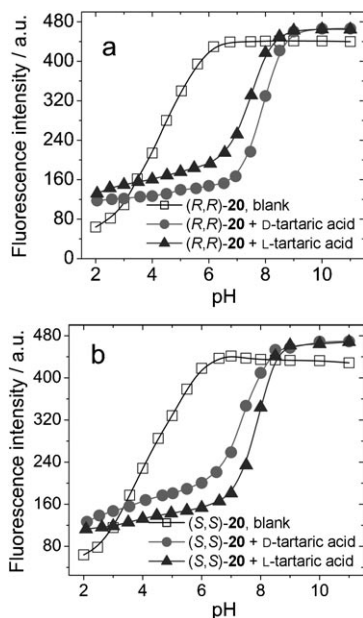


Figure 2. Fluorescence intensity pH profile of a) (R,R)-**20** and b) (S,S)-**20** in the presence of D-/L-tartaric acid, 5.0×10^{-7} mol dm⁻³ of sensors in methanol/water mixed solvent (3:1 v/v). $\lambda_{\text{ex}} = 375$ nm, $\lambda_{\text{em}} = 488$ nm, [D-/L-tartaric acid] = 0.01 mol dm⁻³, 20 °C.

orophore as the electron acceptor of PET), however, the emission is intensified at acidic pH but diminished at basic pH, due to the protonation of the amine N atom at acidic pH and the suppression of the PET process (quenching effect). Furthermore, the contrast ratio, or the PET efficiency, of **20** is approximately 6.0 (the emission is intensified by around sixfold upon termination the PET effect), which is a significant improvement compared to the d-PET boronic acid sensors reported by us previously (the contrast ratio of sensor **10** is around 2.0, Scheme 1).^[25f-h] Apparent pK_a values of 4.37 ± 0.89 and 4.32 ± 0.09 were observed for (R,R)-**20** and (S,S)-**20**, respectively.

Previously we reported a d-PET fluorescent boronic acid sensor (sensor **10**, Scheme 1). However, we found that the d-PET effect vanished upon attaching a phenylethynyl moiety to the carbazole fluorophore (sensor **12**, Scheme 1) due to the electron-deficient ethynylene group.^[25g] In contrast, for ethynylated phenothiazine sensor **20**, when an ethynyl group is incorporated, the d-PET effect is retained. Furthermore, we found that the amine precursor of sensor **20** shows the d-PET effect (see the Supporting Information). With carbazole fluorophore, however, the boronic acid subunit as an extra electron-withdrawing substituent is required for the d-PET effect, that is, the amine precursor of the carbazole-based sensor shows the normal a-PET effect.^[25g] Thus we propose the phenothiazine moiety is a stronger electron donor than the carbazole moiety to assemble d-PET fluores-

cent sensors. This finding will be very helpful for the future design of d-PET fluorescent chemosensors.

pH titration of the sensors in presence of D- and L-tartaric acids was carried out (Figure 2). The emission was enhanced in the acidic region; however, a significant reduction in emission was observed in the neutral pH region in the presence of tartaric acid. We found that both the fluorescence enhancement at acidic pH and the diminishment at basic pH is enantioselective, that is, the response of the sensor was different towards the D- or the L- tartaric acids. A mirrored effect was observed for (S,S)-**20** (Figure 2b). In the presence of D- and L-tartaric acids, the apparent pK_a of (R,R)-**20** changed to 7.86 ± 0.14 and 7.34 ± 0.06 , respectively (Figure 2a). With (S,S)-**20**, however, the profile reversed, with apparent pK_a of 7.29 ± 0.07 and 7.78 ± 0.06 being observed for (S,S)-**20** in the presence of D- and L-tartaric acid, respectively.

The binding constants of the sensors with tartaric acid were determined at pH 3.0, 7.0, and 8.0 (Figure 3). At pH 3.0, the emission response of the sensors was enantioselective toward D- and L-tartaric acid and the profile was mirrored. For example, the fluorescence enhancement of sensor **20** was higher toward L-tartaric acid than towards D-tartaric

acid and the profile was reversed with (R,R)-**20**. With (R,R)-**20**, the binding constants toward D- and L-tartaric acid were $k_D = (2.21 \pm 0.19) \times 10^5 \text{ M}^{-1}$ and $k_L = (3.80 \pm 0.70) \times 10^4 \text{ M}^{-1}$, respectively. Thus the enantioselectivity is $k_D/k_L = 5.8:1$. Furthermore, the fluorescence enhancement was more significant with L-tartaric acid. With (S,S)-**20**, however, the response profile was reversed, that is, $k_D = (5.61 \pm 0.46) \times 10^4 \text{ M}^{-1}$ and $k_L = (2.71 \pm 0.26) \times 10^5 \text{ M}^{-1}$, respectively. Thus with (S,S)-**20** the enantioselectivity was switched to $k_D/k_L = 1:4.8$. The fluorescence enhancement was more significant with D-tartaric acid.

Enantioselectivity was observed at pH 7.0. For example, the binding constant of (R,R)-**20** toward L- and D-tartaric acid was $k_L = (8.64 \pm 1.61) \times 10^4 \text{ M}^{-1}$ and $k_D = (2.11 \pm 0.21) \times 10^5 \text{ M}^{-1}$, respectively. Thus the enantioselectivity was $k_L/k_D = 1:2.4$. With (S,S)-**20**, the binding constant toward L- and D-tartaric acid was $k_L = (3.77 \pm 0.23) \times 10^5 \text{ M}^{-1}$ and $k_D = (6.10 \pm 0.82) \times 10^4 \text{ M}^{-1}$, respectively; $k_L/k_D = 6.2:1$. Enantioselectivity was observed for recognition at pH 8.0.

These enantioselectivity values are much higher than the previous d-PET chiral boronic acid based on carbazole,^[25f] for which the enantioselectivity (k_L/k_D) is less than 2.0. Furthermore, a chiral boronic acid a-PET sensor based on anthracene failed to recognize tartaric acid at acidic pH.^[25b] Based on the structural motif of the sensors, we propose that 1:1 binding—that is, formation of the cyclic binding complexes—is responsible for the enantioselectivity.^[25b]

To validate the enantioselectivity of sensor **20** toward D- and L-tartaric acids, we studied the recognition of D- and L-mandelic acid with **20** (see the Supporting Information, Figure S62). Based on our previous study,^[25a-d,f] no enantioselectivity should be observed for the recognition of D- and L-mandelic acids with bisboronic acid **20** because the mandelic acids have one α -hydroxyl carboxylic acid unit and thus can interact with only one of the two binding sites of the bisboronic acid sensor **20**. On the contrary, tartaric acid can interact with the two binding sites of the bisboronic acid sensor **20** simultaneously).

With (R,R)-**20**, binding constants of $(6.97 \pm 0.68) \times 10^2 \text{ M}^{-1}$ and $(7.07 \pm 0.96) \times 10^2 \text{ M}^{-1}$ were obtained for the D- and L-mandelic acid, respectively, thus the enantioselectivity was close to 1:1. Furthermore, the apparent pK_a of the (R,R)-**20** changed from 4.29 ± 0.08 to 6.87 ± 0.03 or 6.94 ± 0.02 in the presence of D- or L-mandelic acid, respectively. All these results indicate that there is no enantioselectivity for the recognition of mandelic acid. Furthermore, the binding constants of mandelic acids with **20** are around 100 or 1000 times lower than those obtained for tartaric acid. The lower binding constant of mandelic acid is due to the formation of the noncyclic 1:2 binding complexes, which are devoid of the synergetic effect of the 1:1 cyclic complexation that enhances binding.^[25a,b,f] This result indicates that the enantioselectivity observed for recognition of tartaric acid with **20** (Figure 2 and Figure 3) is due to the formation of a cyclic 1:1 binding complex.^[25a,b,f]

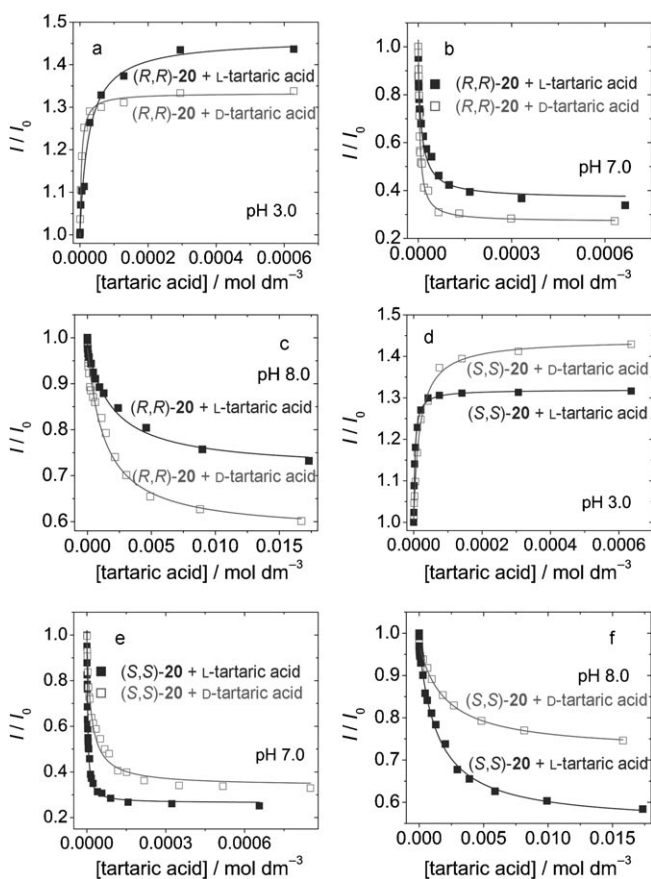


Figure 3. Relative fluorescence intensity of (R,R)-**20** and (S,S)-**20** versus concentration of D-/L-tartaric acid: a) (R,R)-**20**, pH 3.0; b) (R,R)-**20**, pH 7.0; c) (R,R)-**20**, pH 8.0; d) (S,S)-**20**, pH 3.0; e) (S,S)-**20**, pH 7.0; f) (S,S)-**20**, pH 8.0. $\lambda_{\text{ex}} = 375 \text{ nm}$, $\lambda_{\text{em}} = 520 \text{ nm}$, $5.0 \times 10^{-7} \text{ mol dm}^{-3}$ of sensors in MeOH/H₂O mixed solvent 3:1 v/v, 20 °C.

Chiral bisboronic acid sensor with a larger binding pocket—

Application of the modular approach: The potential of our modular strategy to assemble chiral molecular sensors was demonstrated by the preparation of sensor **25** (Scheme 3) with a larger scaffold than sensor **20** (Scheme 2). With the Sonogashira coupling reaction, the binding pocket of **20** was increased and (*S,S*)-**25** and (*R,R*)-**25** was obtained (Scheme 3). To control the binding pocket and not generate too large of a binding pocket (otherwise recognition of small analytes such as tartaric acid would be difficult), we used the *meso*-substituted 3-bromobenzaldehyde to construct the sensor (Scheme 3). It should be noted that the distance between the N atom (PET switch) and the fluorophore core is larger than that in sensor **20** (Scheme 2).

Interestingly, even with extra ethynylene moiety, up to an eightfold enhancement was observed for the d-PET effect for **25** (Figure 4). This result indicates that phenothiazine is

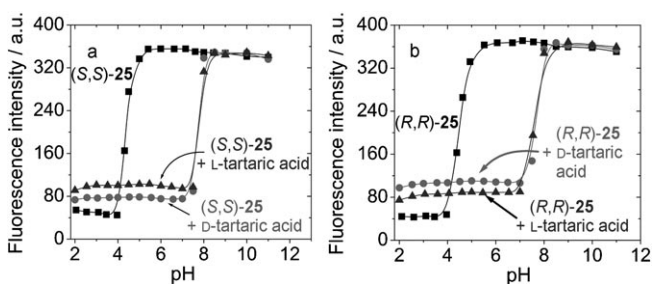


Figure 4. Fluorescence intensity pH profile of a) (*S,S*)-**25** and b) (*R,R*)-**25** in the presence of D-/L-tartaric acids, $5.0 \times 10^{-7} \text{ mol dm}^{-3}$ of sensors in MeOH/H₂O mixed solvent 3:1 v/v. $\lambda_{\text{ex}} = 380 \text{ nm}$, $\lambda_{\text{em}} = 490 \text{ nm}$, [D-/L-tartaric acid] = 0.01 mol dm^{-3} , 20 °C.

a much stronger electron donor than carbazole. Our findings will be helpful for the design of d-PET fluorescent chemosensors.

Compared to sensor **20**, the detection window of **25** (the area between the blank pH titration curve and the titration curve in the presence of analytes) is increased (Figure 4). The apparent $\text{p}K_{\text{a}}$ of the (*S,S*)-**25** and (*R,R*)-**25** are 4.35 ± 0.11 and 4.43 ± 0.11 , respectively. In the presence of tartaric acid, the apparent $\text{p}K_{\text{a}}$ increased substantially. For example, the $\text{p}K_{\text{a}}$ of (*S,S*)-**25** was increased to 7.86 ± 0.14 and 7.78 ± 0.14 in the presence of L-tartaric acid and D-tartaric acid, respectively.

The emission of **25** in solvents with different polarity was also investigated (see the Supporting Information, Figure S46). We found that the emission is not diminished in protic solvents, such as methanol or the aqueous buffer. These photophysical parameters are ideal for application in fluorescent molecular sensor design.

Enantioselective recognition of tartaric acid with sensor **25** was observed at pH 4.0 (Figure 5a and b). For example, the emission enhancement of (*S,S*)-**25** toward L- and D-tartaric acid is 2.2-fold and 1.4-fold, respectively (Figure 5a). With (*R,R*)-**25**, the response profile reversed (Figure 5b), and the emission enhancement towards L- and D-tartaric acid are 1.4-fold and 1.9-fold, respectively.

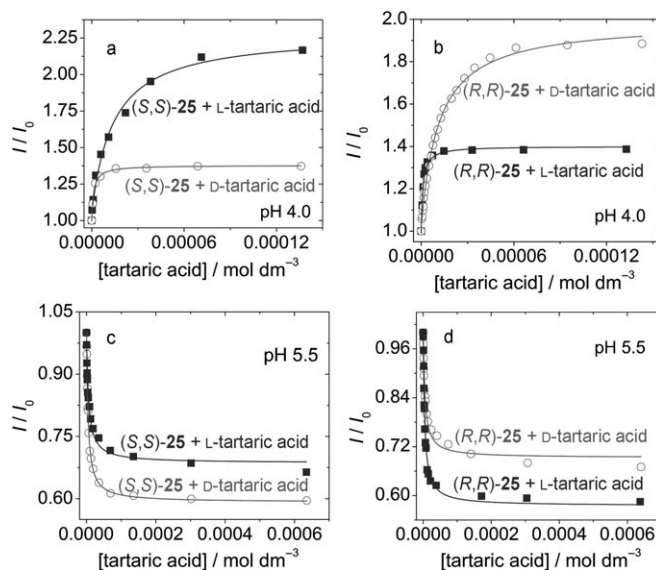


Figure 5. Relative fluorescence intensity of sensors **25** versus concentration of D- and L-tartaric acid. a) (*S,S*)-**25**, pH 4.0; b) (*R,R*)-**25**, pH 4.0; c) (*S,S*)-**25**, pH 5.5; d) (*R,R*)-**25**, pH 5.5. $\lambda_{\text{ex}} = 380 \text{ nm}$, $\lambda_{\text{em}} = 500 \text{ nm}$, $5.0 \times 10^{-7} \text{ mol dm}^{-3}$ of sensors **25** in MeOH/H₂O mixed solvent (MeOH/H₂O = 3:1 v/v), 20 °C.

Enantioselectivity was also found for the binding constants. For example, the binding constants of (*S,S*)-**25** toward D- and L-tartaric acid are $k_{\text{D}} = (7.83 \pm 0.76) \times 10^5 \text{ M}^{-1}$ and $k_{\text{L}} = (7.15 \pm 1.11) \times 10^4 \text{ M}^{-1}$, respectively. Thus the enantioselectivity is $k_{\text{D}}/k_{\text{L}} = 11.0:1$. With (*R,R*)-**25**, the selectivity was reversed, binding constants toward D- and L-tartaric acid are $k_{\text{D}} = (8.90 \pm 0.41) \times 10^4 \text{ M}^{-1}$ and $k_{\text{L}} = (9.34 \pm 1.08) \times 10^5 \text{ M}^{-1}$, respectively. Thus the enantioselectivity is $k_{\text{D}}/k_{\text{L}} = 1:10.5$. The enantioselectivity is higher than that of sensor **20**. We propose that the enhanced recognition of tartaric acid with sensor **25** is due to the increased size of the binding pocket. Herein we noticed that there is no simple correlation between the magnitude of the binding constants (an around tenfold difference between the enantiomers of tartaric acids) and the emission enhancement (an only around 1.5-fold difference in the fluorescence enhancement for the D- and L-tartaric acids). We propose that this discrepancy is due to the complexity of the fluorescence relay (transduction), that is, both tight binding (suppression of the PET effect through direct or indirect B–N interaction) and conformation restriction will enhance the fluorescence.

The binding of **25** with tartaric acids at pH 5.5 was also investigated (Figure 5c and d). No significant enantioselectivity was observed for the binding constants. For example, $k_{\text{D}} = (2.22 \pm 0.11) \times 10^5 \text{ M}^{-1}$ and $k_{\text{L}} = (2.05 \pm 0.22) \times 10^5 \text{ M}^{-1}$ were obtained for (*S,S*)-**25**. We noticed this phenomenon previously,^[25b] but we do not have a clear explanation at the present time. However, the fluorescence diminishment is enantioselective. For example, with (*S,S*)-**25**, the emission diminishment is more significant for D-tartaric acid than L-tartaric acid (Figure 5c). For (*R,R*)-**25**, however, the emission diminishment is more significant with L-tartaric acid than

that with D-tartaric acid. Interaction or geometry restriction may lead to emission enhancement.

We studied the recognition of D- and L-mandelic acids with sensor **25**; no enantioselectivity was observed (Supporting Information, Figures S63 and S64). The binding constants of (*R,R*)-**25** with D- and L-mandelic acid are $(6.86 \pm 1.50) \times 10^3 \text{ M}^{-1}$ and $(6.94 \pm 0.70) \times 10^3 \text{ M}^{-1}$, respectively. Also, no enantioselectivity was observed for the fluorescence diminishment. This result indicates that the enantioselectivity observed for recognition of tartaric acid with sensor **25** is most probably due to the formation of a cyclic 1:1 binding complex.^[25a,b,f]

The effect of the binding pocket size of **20** and **25** on the recognition of sugar acids was also studied (Supporting Information, Figure S47).^[32] For example, **20** gives a small response to D-gluconic acid (the emission of the blank sensor is quenched slightly), but with sensor **25**, a more significant response to D-gluconic acid was observed (the emission of sensor **25** was quenched more significantly). The favored binding of D-gluconic acid by sensor **25** (with a bigger binding pocket than sensor **20**) was also demonstrated by the higher binding constant. For example, a binding constant of $k = (2.04 \pm 0.22) \times 10^3 \text{ M}^{-1}$ was observed with (*S,S*)-**20**. With sensor (*S,S*)-**25**, however, a binding constant of $(5.21 \pm 1.08) \times 10^4 \text{ M}^{-1}$ was observed, which is twentyfold higher than that of (*S,S*)-**20**. Furthermore, no enantioselectivity on D-gluconic acid was observed with sensor **20**. With sensor **25**, however, a 1.5:1 enantioselectivity was observed. This result indicates that the bigger binding pocket of sensor **25** is capable of effective chiral recognition of gluconic acid. The recognition of sugar alcohols with the sensors was also studied. Enantioselectivity was observed for the recognition of the sugar alcohols. The binding constants of the sensors with analytes are summarized in Table 2.

Consecutive fluorescence enhancement/diminishment upon increasing the analyte concentration—Transition of the binding stoichiometry from 1:1 to 1:2: Sequential emission enhancement/diminishment was found for sensor **25** with an increase in the D- and L-tartaric acid concentration (Figure 6). The binding at low tartaric acid concentration

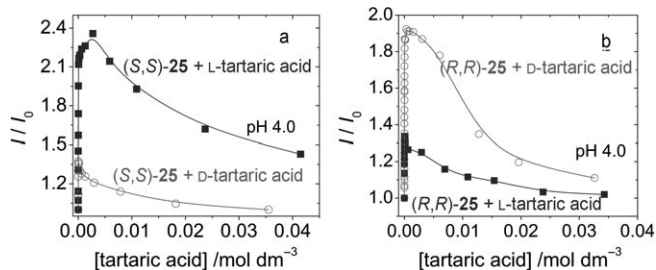


Figure 6. Relative fluorescence intensity of a) (*S,S*)-**25** and b) (*R,R*)-**25** versus the concentration of D- and L-tartaric acid. pH 4.0, $\lambda_{\text{ex}} = 380 \text{ nm}$, $\lambda_{\text{em}} = 500 \text{ nm}$, $5.0 \times 10^{-7} \text{ mol dm}^{-3}$ of sensor **25** in MeOH/H₂O mixed solvent 3:1 v/v, 20 °C.

produces emission enhancement. At higher tartaric acid concentration, however, the emission intensity decreased. We propose the consecutive emission enhancement/diminishment with increasing the tartaric acid concentration at pH 4.0 is due to a change of the binding stoichiometry from 1:1 to 1:2. Previously we observed a similar effect with the BINOL-based chiral sensor **1** (Scheme 1).^[25a]

With **20**, however, no emission enhancement/diminishment was observed. Thus we propose that the small binding pocket of sensor **20** is the correct molecular size for tartaric acid, and thus 1:1 binding is the favored stoichiometry. This was demonstrated by our previous experiments with the an-

Table 2. Binding constants of the chiral bis-boronic acid sensors **20** and **25** with analytes.

Analytes	pH	(<i>S,S</i>)- 20	(<i>R,R</i>)- 20	(<i>S,S</i>)- 25	(<i>R,R</i>)- 25
D-tartaric acid	3.0	$(5.61 \pm 0.46) \times 10^4$ (↑)	$(2.21 \pm 0.19) \times 10^5$ (↑)	— ^[b]	— ^[b]
	4.0	— ^[b]	— ^[b]	$(7.83 \pm 0.76) \times 10^5$ (↑)	$(8.90 \pm 0.41) \times 10^4$ (↑)
	5.5	— ^[b]	— ^[b]	$(2.22 \pm 0.11) \times 10^5$ (↓)	$(1.98 \pm 0.18) \times 10^5$ (↓)
	7.0	$(6.10 \pm 0.82) \times 10^4$ (↓)	$(2.11 \pm 0.21) \times 10^5$ (↓)	— ^[b]	— ^[b]
	8.0	$(5.00 \pm 1.04) \times 10^2$ (↓)	$(7.31 \pm 1.04) \times 10^2$ (↓)	— ^[b]	— ^[b]
L-tartaric acid	3.0	$(2.71 \pm 0.26) \times 10^5$ (↑)	$(3.80 \pm 0.70) \times 10^4$ (↑)	— ^[b]	— ^[b]
	4.0	— ^[b]	— ^[b]	$(7.15 \pm 1.11) \times 10^4$ (↑)	$(9.34 \pm 1.08) \times 10^5$ (↑)
	5.5	— ^[b]	— ^[b]	$(2.05 \pm 0.22) \times 10^5$ (↓)	$(2.28 \pm 0.19) \times 10^5$ (↓)
	7.0	$(3.77 \pm 0.23) \times 10^5$ (↓)	$(8.64 \pm 1.61) \times 10^4$ (↓)	— ^[b]	— ^[b]
	8.0	$(7.06 \pm 0.58) \times 10^2$ (↓)	$(5.21 \pm 0.75) \times 10^2$ (↓)	— ^[b]	— ^[b]
D-mandelic acid	3.0	— ^[b]	$(6.97 \pm 0.68) \times 10^2$ (↑)	— ^[b]	— ^[b]
	5.5	— ^[b]	— ^[b]	— ^[b]	$(6.86 \pm 1.50) \times 10^3$ (↓)
L-mandelic acid	3.0	— ^[b]	$(7.07 \pm 0.96) \times 10^2$ (↑)	— ^[b]	— ^[b]
	5.5	— ^[b]	— ^[b]	— ^[b]	$(6.94 \pm 0.70) \times 10^3$ (↓)
D-gluconic acid	5.5	— ^[b]	— ^[b]	$(5.21 \pm 1.08) \times 10^4$ (↓)	$(3.58 \pm 0.71) \times 10^4$ (↓)
	7.0	$(2.04 \pm 0.22) \times 10^3$ (↓)	$(2.65 \pm 0.42) \times 10^3$ (↓)	— ^[b]	— ^[b]
D-sorbitol	5.5	— ^[b]	— ^[b]	$(2.99 \pm 1.25) \times 10^4$ (↓)	$(2.13 \pm 1.08) \times 10^4$ (↓)
	7.0	$(1.04 \pm 0.11) \times 10^3$ (↓)	$(1.21 \pm 0.10) \times 10^3$ (↓)	— ^[b]	— ^[b]
D-mannitol	7.0	$(1.42 \pm 0.25) \times 10^3$ (↓)	$(1.75 \pm 0.31) \times 10^3$ (↓)	$(4.77 \pm 1.96) \times 10^4$ (↓)	$(1.16 \pm 0.34) \times 10^4$ (↓)
D-glucose	7.0	$(1.59 \pm 0.54) \times 10^3$ (↓)	$(1.22 \pm 0.25) \times 10^3$ (↓)	— ^[b]	— ^[b]
xylytol	7.0	$(3.23 \pm 0.60) \times 10^4$ (↓)	$(2.70 \pm 0.56) \times 10^4$ (↓)	— ^[b]	— ^[b]

[a] Fluorescence enhancement (↑) or diminishment (↓) in the presence of analytes are indicated. [b] Not determined due to the weak fluorescence response at the specific pH, indicated by the pH titrations.

thracene-based chiral boronic acid sensor **2** (Scheme 1). For sensor **20**, the binding with tartaric acid is tight, thus 1:1 binding is favored. For sensor **25**, however, 1:2 binding becomes dominant at high tartaric acid concentrations.

To prove the transition of the binding stoichiometry from 1:1 to 1:2, we measured the mass spectra of sensor (*S,S*)-**25**/tartaric acid solutions (Supporting Information, Figures S39–S41). The 1:1 binding complex of (*S,S*)-**25**/D-tartaric acid (m/z 1254.3344, adduct with Na^+) (with a dual-MeOH-inserted, zwitterionic, intramolecular hydrogen-bond structure, Figure S41) was found for the 1:1 (*S,S*)-**25**/D-tartaric acid ratio (Supporting Information, Figures S39 and S41). By increasing the ratio of D-tartaric acid to 10:1 (over (*S,S*)-**25**), a partially opened structure (m/z 1200.3722) was observed. A further increase of the ratio of the mixture (100:1) resulted in the appearance of the opened form (1:2 binding complex) with m/z 1318.3667. Although some irregularities exist in the mass spectroscopic analysis, the trend of the binding stoichiometry transition from 1:1 to 1:2 upon increasing the ratio of tartaric acid is clear. Unfortunately, attempts to grow single crystals to support these assumptions failed.

Rationalization of the d-PET effect of the chiral fluorescent boronic acid sensors—DFT/time-dependent (TD)-DFT calculations: Recently, DFT/TD-DFT calculations have been used for investigation of the photophysics of fluorophores and fluorescent molecular sensors.^[33–35] Previously we used DFT/TD-DFT calculations to study d-PET fluorescent boronic acid sensors^[25g,h] as well as fluorescent OFF/ON thiol probes.^[36,37]

The strategy we employed is to examine the property of the lowest-lying singlet excited state (S_1), which is responsible for the fluorescence emission (Kasha's rule).^[38] The S_1 state of the protonated form of the d-PET boronic acid sensor **10** (Scheme 1) is a dark state (with $S_0 \rightarrow S_1$ oscillator strength close to zero). Thus the $S_0 \rightarrow S_1$ is a forbidden transition, as well as the $S_1 \rightarrow S_0$ transition. Therefore the protonated form of the d-PET boronic acid sensors produce a weak emission (at acidic pH). For the neutral form of the d-PET sensors, however, the $S_0 \rightarrow S_1$ oscillator strength increases significantly, thus $S_0 \rightarrow S_1$ is an allowed transition and the sensor is probably fluorescent ($S_1 \rightarrow S_0$ is allowed). Therefore, an intensified emission at neutral pH will be observed.^[25f,g]

For the protonated **25** (Figure 7), we observed a charge-transfer character for the HOMO \rightarrow LUMO transition. The S_1 state of protonated **25** is a dark state ($f=0.0042$), but the S_1 state of neutral **25** is probably a radiative state ($f=0.69$), indicates an allowed $S_0 \rightarrow S_1$ transition, thus S_1 is probably a radiative state and the sensor is probably fluorescent; see the Supporting Information, Table S1). Therefore, we propose that the neutral sensor **25** will display a stronger emission than the protonated form. This prediction is fully supported by the experimental results.

Recognition of disaccharides and glycosylated steroids: Polysaccharides and glycosylated steroids are biologically important. For example, some oligosaccharides are responsi-

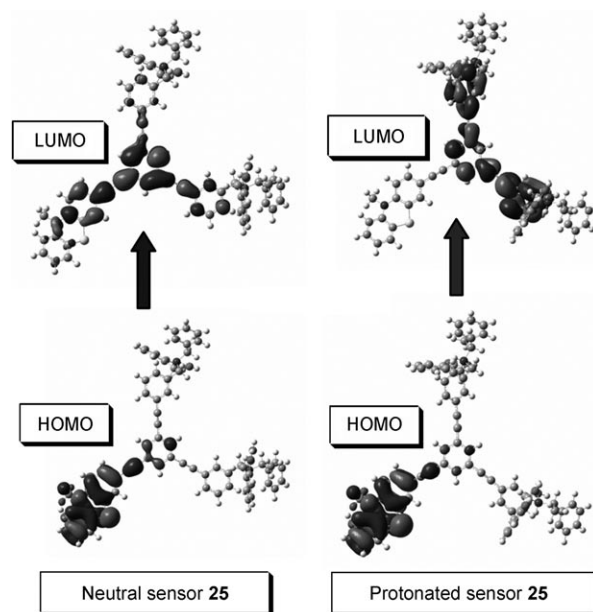


Figure 7. Frontier molecular orbitals of neutral and protonated sensor **25**. Note the HOMO and LUMO of the neutral **25** is localized on the phenothiazine unit, whereas the HOMO \rightarrow LUMO transition of protonated **25** is an electron-transfer process from the ethynylated phenothiazine framework. Calculated with DFT methods on the B3LYP/3-21G level.

ble for cell recognition. Thus recognition of polysaccharides with fluorescent molecular sensors is significant.^[39–41] The binding pockets of the sensors, especially sensor **25**, are large, therefore the binding of a monosaccharide, such as glucose, is not tight. For (*R,R*)-**25** and (*S,S*)-**25**, no significant binding was observed. We suppose that binding with disaccharides may be tight for the sensors. Thus the disaccharides of sucrose, lactose, and maltose were tested against the sensors. We observed stronger binding than that with glucose. The binding constants are usually up to 10^4 M^{-1} scale.

Enantioselectivity, demonstrated by both the fluorescence response and binding constants, was observed for the sensors. For example, the (*S,S*)-**25** and (*R,R*)-**25** gives similar response to lactose. Binding constants of $(8.31 \pm 2.92) \times 10^3 \text{ M}^{-1}$ and $(5.05 \pm 0.84) \times 10^3 \text{ M}^{-1}$ were found for the (*S,S*)-**25** and (*R,R*)-**25**, respectively (Figure 8a). With maltose, however, (*R,R*)-**25** and (*S,S*)-**25** give drastically different responses.

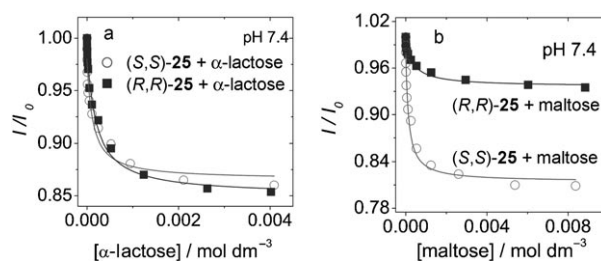


Figure 8. Fluorescent recognition of the α -lactose and maltose. a) and b) Relative fluorescence intensity of (*R,R*)-**25** and (*S,S*)-**25** versus the concentration of α -lactose and maltose. $\lambda_{\text{ex}}=380 \text{ nm}$, $\lambda_{\text{em}}=500 \text{ nm}$, $5.0 \times 10^{-7} \text{ mol dm}^{-3}$ of sensor in MeOH/ H_2O mixed solvent (MeOH/ $\text{H}_2\text{O}=3:1 \text{ v/v}$), 20°C .

Table 3. Apparent association constants (K_a) [M^{-1}] of sensors **20** and **25** with different disaccharides and ginsenosides **Re** and **Rb1**.^[a]

Analytes	(<i>S,S</i>)- 20	(<i>R,R</i>)- 20	(<i>S,S</i>)- 25	(<i>R,R</i>)- 25
sucrose	$(4.01 \pm 1.08) \times 10^4$ (↓)	$(6.28 \pm 1.79) \times 10^4$ (↓)	$(2.50 \pm 0.41) \times 10^4$ (↓)	$(3.10 \pm 1.30) \times 10^4$ (↓)
α -lactose	$(1.19 \pm 0.39) \times 10^4$ (↓)	$(3.45 \pm 1.11) \times 10^4$ (↓)	$(8.31 \pm 2.92) \times 10^3$ (↓)	$(5.05 \pm 0.84) \times 10^3$ (↓)
maltose	$(1.03 \pm 0.45) \times 10^4$ (↓)	$(2.19 \pm 0.83) \times 10^5$ (↓)	$(7.18 \pm 1.78) \times 10^3$ (↓)	$(2.48 \pm 0.56) \times 10^3$ (↓)
ginsenosides Re	$(5.94 \pm 0.57) \times 10^5$ (↓)	$(5.11 \pm 0.82) \times 10^5$ (↓)	$(6.79 \pm 0.50) \times 10^5$ (↓)	$(1.95 \pm 0.31) \times 10^5$ (↓)
ginsenosides Rb1	$(6.91 \pm 0.62) \times 10^5$ (↓)	$(5.34 \pm 1.18) \times 10^5$ (↓)	$(2.88 \pm 0.51) \times 10^6$ (↓)	$(1.81 \pm 0.32) \times 10^6$ (↓)

[a] Binding studies were conducted in MeOH/H₂O mixed solvent (MeOH/H₂O = 3:1 v/v), pH 7.4. Fluorescence enhancement (↑) or diminishment (↓) in the presence of analytes are indicated.

For example, the fluorescence decrease of (*S,S*)-**25** in the presence of maltose is around 16%. With (*R,R*)-**25**, however, the emission decrease is only 5%. Furthermore, the binding constants of (*R,R*)-**25** and (*S,S*)-**25** with maltose is $(7.18 \pm 1.78) \times 10^3 M^{-1}$ and $(2.48 \pm 0.56) \times 10^3 M^{-1}$, respectively (Figure 8b). Enantioselectivities were also found for (*S,S*)-**20** and (*R,R*)-**20** (Supporting Information). The bindings of **20** and **25** with disaccharides are summarized in Table 3. The binding constants are generally much higher than recently reported bis-boronic acid sensors for the detection of saccharides, including maltose and lactose (typically less than $500 M^{-1}$).^[40b]

The binding pockets of **20** and **25** are large, therefore we studied their interaction with large analytes such as glycosylated steroids. Herein we used ginsenosides, which are believed to be responsible for the physiological benefits of ginseng, one of the most widely taken medical herbs. Current analysis of ginsenosides requires sophisticated instruments, such as HPLC analysis. To the best of our knowledge, fluorescent chemosensors are rarely used for recognition of ginsenosides.^[40a]

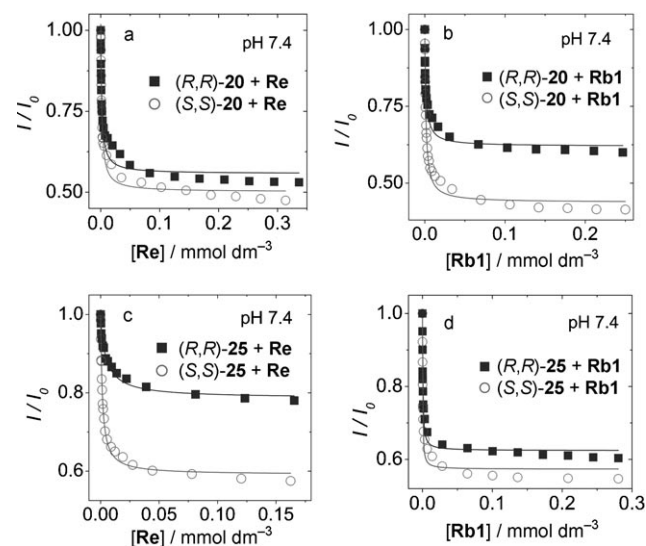


Figure 9. Fluorescent recognition of the ginsenosides **Re** and **Rb1**. a) and b) Relative fluorescence intensity of (*R,R*)-**20** and (*S,S*)-**20** versus concentration of **Re** and **Rb1**: $\lambda_{ex} = 375$ nm, $\lambda_{em} = 488$ nm. c) and d) Relative fluorescence intensity of (*R,R*)-**25** and (*S,S*)-**25** versus concentration of **Re** and **Rb1**: $\lambda_{ex} = 380$ nm, $\lambda_{em} = 500$ nm. $5.0 \times 10^{-7} \text{ mol dm}^{-3}$ of sensor in MeOH/H₂O mixed solvent 3:1 v/v, 20 °C.

We found that the emission intensity of the sensors decreased in the presence of ginsenosides **Re** and **Rb1** (ginsenosides are not stable in acidic pH, therefore pH titrations were not carried out; Figure 9). We found that **20** and **25** bind tightly with the ginsenosides. For example, the binding constants are generally

on the scale of $5.0 \times 10^5 M^{-1}$. These binding constants are around two-hundred-fold higher than a porphyrin receptor for ginsenosides.^[40a] We tentatively attribute the tight binding to the good fitting of the ginsenosides to the bis-boronic acid binding pocket of sensors **20** and **25**. Furthermore, we observed enantioselectivity (either by the binding constants or the fluorescence response) for the recognition of the ginsenosides **Re** and **Rb1**. For example, the emission of (*S,S*)-**20** decreases to 42% of the initial intensity in the presence of **Rb1**. With (*R,R*)-**20**, however, the emission decreases to 60%. Similar binding constants were observed for (*R,R*)-**20** and (*S,S*)-**20** with **Rb1**. Enantioselectivity was also found for the recognition of **Re** with sensor **25** (Table 3).

Conclusion

In conclusion, we have devised a new modular approach for the assembly of chiral fluorescent boronic acid sensors, in which the fluorophore, the binding sites, and the chirogenic centers are easily assembled onto a scaffold. This modular approach for the preparation of chiral molecular sensors is in contrast to the previously reported chiral sensors that consist of an integrated fluorophore and chirogenic centers, which are difficult to change into other structures. The ethynylated phenothiazine fluorophore shows visible-light excitation, emission at 492 nm, and large Stokes shift (142 nm); a high fluorescence quantum yield was also found ($\Phi = 0.487$). This makes the ethynylated phenothiazine an ideal fluorophore for fluorescent chemosensor development. In our modular chiral sensors, the fluorophore and the chirogenic center are connected by an ethynylene group ($C \equiv C$), which ensures efficient electron communication between the N atom (PET switch center) and the fluorophore. A high contrast ratio (≈ 8.0) is observed; even the distance between the N atom (PET switch) and the fluorophore core is large. We attribute the high contrast ratio to the strong electron-donating ability of the phenothiazine fluorophore. Furthermore, the chiral boronic acid sensors show a d-PET effect, that is, the fluorophore serves as electron donor in the PET process and the sensors show intensified emission at neutral pH but diminished emission in the acidic pH region, which is in stark contrast to the normal a-PET fluorescent chemosensors. Enantioselective recognition of D- and L-tartaric acid was achieved with the sensors, and the recognition of the analytes is dependent upon the size of the binding

pocket of the boronic acid sensors. The transition of binding stoichiometry from 1:1 (closed form) to 1:2 (nonycyclic open form) upon increasing the tartaric acid concentration was proposed for sensor **25** based on the fluorescence titration (consecutive emission enhancement/diminishment was observed with increasing the tartaric acid concentration) and was supported by the mass spectroscopic analysis. The sensors were used for enantioselective recognition of disaccharides (sucrose, lactose, and maltose) and glycosylated steroids (ginsenosides). Tight binding and selective recognition were found. We believe that the modular structural motif of the fluorescent chiral boronic acid sensor devised by us can be generalized for the preparation of chiral molecular sensors, not limited to boronic acid sensors, with binding sites other than boronic acid groups. This would make it possible to design chiral fluorescent molecular probes in which the fluorophore and the chirogenic center are easily interchangeable so as to tune the emission properties and enantioselectivity of the sensors.

Experimental Section

The fluorescence emission spectra of the sensors were determined as the pH was changed from pH 2 to 11 in approximate intervals of approximately 0.5 pH units. The pH was controlled by using minimum volumes of sodium hydroxide and hydrochloric acid solutions. The boronic acid sensors can form methanol adducts (as indicated by the mass spectral analysis). The fluorescence spectra of the sensors in the presence of the analytes were recorded as increasing amounts of the analyte were added to the solution. All the DFT/TD-DFT calculations were performed using Gaussian 09.^[42]

10-Butyl-10H-phenothiazine (15): $n\text{C}_4\text{H}_9\text{Br}$ (8.2 g, 60 mmol) was added to a stirred solution of phenothiazine (9.95 g, 50 mmol), hexadecyltrimethylammonium bromide (0.5 g), and NaOH (3.0 g) in acetone (50 mL). The mixture was heated to reflux for 6 h. Then the solvent was removed under reduced pressure, the residue was extracted with dichloromethane (CH_2Cl_2), and washed with water. The organic phase was dried over anhydrous Na_2SO_4 . The solvent was removed and the residue was purified by column chromatography (silica gel, CH_2Cl_2 /petroleum ether, 1:3 v/v). Yield: 6.64 g (52%) of a light green liquid. $^1\text{H NMR}$ (CDCl_3 , 400 MHz, TMS): $\delta = 7.10\text{--}7.14$ (m, 4H), 6.86 (t, $J = 7.2$ Hz, 2H), 6.83 (d, $J = 8.4$ Hz, 2H), 3.80 (t, $J = 7.2$ Hz, 2H), 1.73–1.80 (m, 2H), 1.38–1.48 (m, 2H), 0.90 ppm (t, $J = 7.8$ Hz, 3H); atmospheric-pressure chemical ionization (APCI) MS: m/z : calcd for $\text{C}_{16}\text{H}_{17}\text{NS}$: 256.1 [$M+H$]⁺; found: 256.0.

3-Bromo-10-butyl-10H-phenothiazine (16): NaOH (0.66 g, 6.44 mmol, in 40 mL glacial acetic acid) was added to a solution of **15** (1.40 g, 5.48 mmol) in chloroform (10 mL). Then bromine (0.28 mL, 5.48 mmol, in 6 mL glacial acetic acid) was added dropwise at 0 °C. The mixture was stirred at 0–5 °C for 1 h. The solvents were removed. Water (50 mL) and CH_2Cl_2 (100 mL) were added, and the organic layer was dried with MgSO_4 . The solvent was removed, and the residue was purified by column chromatography (silica gel, CH_2Cl_2 /petroleum ether, 1:3 v/v). Yield: 1.28 g (70%) of a light yellow liquid. $^1\text{H NMR}$ (CDCl_3 , 400 MHz, TMS): $\delta = 7.17$ (d, $J = 8.0$ Hz, 2H), 7.06–7.13 (m, 2H), 6.86 (t, $J = 8.0$ Hz, 1H), 6.80 (d, $J = 8.0$ Hz, 1H), 6.60 (t, $J = 8.0$ Hz, 1H), 3.73 (t, $J = 8.0$ Hz, 2H), 1.66–1.75 (m, 2H), 1.35–1.45 (m, 2H), 0.88 ppm (t, $J = 8.0$ Hz, 3H); APCI-MS: m/z : calcd for $\text{C}_{16}\text{H}_{16}\text{BrNS}$: 335.3 [$M+H$]⁺; found: 335.1.

10-Butyl-3-ethynyl-10H-phenothiazine (17): [$\text{PdCl}_2(\text{PPh}_3)_2$] (124.0 mg, 0.17 mmol), PPh_3 (46.5 mg, 0.17 mmol), CuI (33.7 mg, 0.17 mmol), and ethynyltrimethylsilane (435.0 mg, 4.43 mmol) were successively added to a degassed solution of **16** (1.48 g, 4.43 mmol) in dry Et_3N (8 mL) and THF (5 mL). The reaction mixture was heated to reflux under N_2 for 6 h.

Then K_2CO_3 (1.65 g, 12 mmol) and methanol (5 mL) were added, and the solution was stirred for 1 h at room temperature. The solvents were removed under reduced pressure. The residue was taken up with CH_2Cl_2 and washed with water. The organic layer was dried over MgSO_4 . After the solvent was removed, the residue was purified by column chromatography (silica gel, CH_2Cl_2 /petroleum ether, 1:6 v/v). Yield: 1.04 g (84%) of a yellow liquid. $^1\text{H NMR}$ (CDCl_3 , 400 MHz, TMS): $\delta = 7.23$ (m, 2H), 7.09–7.16 (m, 2H), 6.90 (t, $J = 8.0$ Hz, 1H), 6.84 (d, $J = 8.0$ Hz, 1H), 6.75 (d, $J = 8.4$ Hz, 1H), 3.81 (t, $J = 7.2$ Hz, 2H), 3.03 (s, 1H), 1.73–1.80 (m, 2H), 1.40–1.49 (m, 2H), 0.92 ppm (t, $J = 8.4$ Hz, 3H); APCI-MS: m/z : calcd for $\text{C}_{18}\text{H}_{17}\text{NS}$: 280.1 [$M+H$]⁺; found: 280.0.

Compound 18: [$\text{Pd}(\text{PPh}_3)_4$] (46.8 mg, 0.04 mmol), CuI (7.7 mg, 0.04 mmol), and **17** (0.35 g, 1.35 mmol) were successively added to a degassed solution of 2-iodo-1,4-benzenedicarboxaldehyde (0.37 g, 1.35 mmol) in dry Et_3N (5 mL) and THF (3.0 mL). The mixture was heated to reflux under nitrogen for 8 h. The solvents were removed. The residue was washed with water and CH_2Cl_2 . The organic layer was dried over MgSO_4 . After the solvent was removed, the residue was purified by column chromatography (silica gel, CH_2Cl_2 /petroleum ether, 3:1 v/v). Yield: 0.22 g (40%) of a red oil. $^1\text{H NMR}$ (CDCl_3 , 400 MHz, TMS): $\delta = 10.65$ (s, 1H), 10.07 (s, 1H), 8.03–8.07 (m, 2H), 7.85 (d, $J = 8.0$ Hz, 1H), 7.26–7.35 (m, 2H), 7.10–7.18 (m, 2H), 6.92 (t, $J = 8.0$ Hz, 1H), 6.86 (d, $J = 8.0$ Hz, 1H), 6.80 (d, $J = 8.0$ Hz, 1H), 3.83 (t, $J = 8.0$ Hz, 2H), 1.75–1.82 (m, 2H), 1.44–1.49 (m, 2H), 0.93 ppm (t, $J = 8.0$ Hz, 3H); $^{13}\text{C NMR}$ (100 MHz, CDCl_3): $\delta = 191.1, 190.9, 146.5, 144.3, 139.4, 138.8, 134.6, 131.2, 130.3, 128.2, 128.0, 127.9, 127.5, 127.4, 125.1, 123.9, 123.0, 115.7, 115.2, 115.1, 97.8, 83.9, 47.3, 28.9, 20.1, 13.8, 0$ ppm; TOF-MS (EI)⁺: m/z : calcd for $\text{C}_{26}\text{H}_{21}\text{NO}_2\text{S}$: 411.1293 [$M+H$]⁺; found: 411.1302.

Compound (S,S)-19: (S)-1-Phenylethanamine (0.17 g, 1.46 mmol) was added to a solution of **18** (0.02 g, 0.49 mmol) in dry THF (3 mL). The reaction mixture was heated to reflux under nitrogen for 8 h. After the solution was cooled to RT, $\text{NaBH}_3(\text{CN})$ (0.15 g, 2.45 mmol) was added in several portions to the stirred solution, and the stirring was continued for 1 h. The resulting mixture was evaporated to dryness. The residual was purified by column chromatography (silica gel, CH_2Cl_2 /MeOH, 30:1 v/v). Yield: 0.12 g (40%) of a yellow oil. $^1\text{H NMR}$ (CDCl_3 , 400 MHz, TMS): $\delta = 7.11\text{--}7.47$ (m, 17H), 6.91 (t, $J = 8.0$ Hz, 1H), 6.85 (d, $J = 8.0$ Hz, 1H), 6.77 (d, $J = 8.0$ Hz, 1H), 3.54–3.89 (m, 8H), 1.75–1.83 (m, 2H), 1.32–1.49 (m, 8H), 0.93 ppm (t, $J = 8.0$ Hz, 3H); TOF-MS (EI)⁺: m/z : calcd for $\text{C}_{42}\text{H}_{43}\text{N}_3\text{S}$: 622.3256 [$M+H$]⁺; found: 622.3275.

Compound (R,R)-19: This compound was synthesized by using a procedure similar to that of (S,S)-19. Yellow oil was obtained with a yield of 36%. $^1\text{H NMR}$ (CDCl_3 , 400 MHz, TMS): $\delta = 7.13\text{--}7.43$ (m, 17H), 6.92 (t, $J = 8.0$ Hz, 1H), 6.86 (d, $J = 8.0$ Hz, 1H), 6.78 (d, $J = 8.0$ Hz, 1H), 3.55–3.88 (m, 8H), 1.76–1.83 (m, 2H), 1.38–1.52 (m, 8H), 0.93 ppm (t, $J = 8.0$ Hz, 3H); TOF-MS (EI)⁺: m/z : calcd for $\text{C}_{42}\text{H}_{43}\text{N}_3\text{S}$: 622.3256 [$M+H$]⁺; found: 622.3285.

Sensor (S,S)-20: (S,S)-**19** (100.0 mg, 0.16 mmol), 2-(2-bromomethylphenyl)-1,3,2-dioxaborinane (138.0 mg, 0.54 mmol), and K_2CO_3 (132.0 mg, 0.96 mmol) were mixed in dry MeCN (5.0 mL). Then the mixture was heated to reflux for 10 h under N_2 . The reaction mixture was cooled to room temperature and diluted HCl was added. Then the mixture was stirred for a further 1 h. The solvent was removed under vacuum, and CH_2Cl_2 was added to take up the residue. The organic layer was washed with water and dried over anhydrous MgSO_4 . The solvent was removed under reduced pressure and the residue was purified by column chromatography (silica gel, CH_2Cl_2 /MeOH, 30:1 v/v). Yield: 40.0 mg (28%) of a light yellow powder. M.p. 205–206 °C; $[\alpha]_{\text{D}}^{20} = (-16.9 \pm 1.0)^\circ$ ($c = 0.11$ in CH_2Cl_2); $^1\text{H NMR}$ (CDCl_3 , 400 MHz): $\delta = 7.75$ (s, 2H), 7.08–7.41 (m, 23H), 6.94 (t, $J = 7.6$ Hz, 1H), 6.89 (d, $J = 8.0$ Hz, 1H), 6.82 (d, $J = 8.0$ Hz, 1H), 4.02–4.10 (m, 2H), 3.86–3.93 (m, 5H), 3.55–3.64 (m, 5H), 1.78–1.85 (m, 2H), 1.57 (d, $J = 8.0$ Hz, 6H), 1.45–1.54 (m, 2H), 0.95 ppm (t, $J = 8.0$ Hz, 3H); $^{13}\text{C NMR}$ (100 MHz, $\text{CDCl}_3/\text{CD}_2\text{OD}$): $\delta = 145.5, 144.7, 141.7, 141.6, 136.4, 135.9, 133.0, 131.2, 130.6, 130.0, 129.6, 129.4, 129.3, 129.0, 128.2, 128.1, 127.7, 127.5, 127.2, 127.0, 124.9, 124.2, 123.3, 122.8, 116.9, 115.6, 115.1, 93.3, 87.8, 58.4, 57.4, 53.1, 50.9, 47.3, 29.0, 20.1, 15.9, 15.6, 13.7$ ppm; TOF-MS (EI)⁺: m/z : calcd for $\text{C}_{58}\text{H}_{61}\text{B}_2\text{N}_3\text{O}_4\text{S}$: 459.7363 [$M+2\text{MeOH}-2\text{H}_2\text{O}+2\text{H}$]⁺; found: 459.7363.

Sensor (R,R)-20: This compound was synthesized by using a procedure similar to that of (S,S)-20. A light-yellow powder was obtained in a yield of 30%. M.p. 205–206 °C. $[\alpha]_D^{25} = (+17.9 \pm 0.7)^\circ$ ($c = 0.11$ in CH_2Cl_2); $^1\text{H NMR}$ (CDCl_3 , 400 MHz): $\delta = 7.60$ (s, 2H), 6.91–7.25 (m, 23H), 6.78 (t, $J = 8.0$ Hz, 1H), 6.74 (d, $J = 8.0$ Hz, 1H), 6.67 (d, $J = 8.0$ Hz, 1H), 3.71–3.78 (m, 5H), 3.37–3.52 (m, 5H), 3.09–3.25 (m, 2H), 1.63–1.70 (m, 2H), 1.41–1.46 (m, 6H), 1.31–1.39 (m, 2H), 0.80 ppm (t, $J = 8.0$ Hz, 3H); $^{13}\text{C NMR}$ (100 MHz, $\text{CDCl}_3/\text{CD}_3\text{OD}$): $\delta = 145.6$, 144.7, 133.0, 131.2, 130.6, 129.9, 129.6, 129.5, 129.3, 129.1, 128.3, 127.7, 127.5, 127.2, 124.9, 124.2, 122.8, 116.9, 115.6, 115.1, 93.3, 87.8, 58.5, 57.4, 53.1, 50.9, 47.3, 29.0, 20.1, 15.9, 15.6, 13.8 ppm; TOF-MS (EI) $^+$: m/z : calcd for $\text{C}_{58}\text{H}_{61}\text{B}_2\text{N}_3\text{O}_4\text{S}$: 459.7363 $[\text{M}+2\text{MeOH}-2\text{H}_2\text{O}+2\text{H}]^{2+}$; found: 459.7359.

3-Ethynylbenzaldehyde (21): [$\text{PdCl}_2(\text{PPh}_3)_2$] (382.0 mg, 0.54 mmol), CuI (104.0 mg, 0.54 mmol), and ethynyltrimethylsilane (3.2 g, 33.0 mmol) were successively added to a degassed solution of 3-bromobenzaldehyde (5.0 g, 27.2 mmol) in dry Et_3N (10 mL) and THF (5 mL). The reaction mixture was heated to reflux under N_2 for 6 h. Then K_2CO_3 (3.7 g, 27.2 mmol) and methanol (10 mL) were added, and the solution was stirred for 1 h at room temperature. The solvents were removed under reduced pressure. The residue was taken up with CH_2Cl_2 and washed with water. The organic layer was dried over MgSO_4 . After the solvent was removed, the residue was purified by column chromatography (silica gel, $\text{CH}_2\text{Cl}_2/\text{petroleum ether}$, 2:1 v/v). Yield: 2.9 g (81%) of a yellow solid. $^1\text{H NMR}$ (CDCl_3 , 400 MHz, TMS): $\delta = 10.00$ (s, 1H), 7.99 (s, 1H), 7.85 (d, $J = 7.6$ Hz, 1H), 7.72 (d, $J = 7.6$ Hz, 1H), 7.49 (t, 1H, $J = 7.6$ Hz), 3.17 ppm (s, 1H).

Compound 22: [$\text{PdCl}_2(\text{PPh}_3)_2$] (450.0 mg, 0.64 mmol), CuI (73.0 mg, 0.39 mmol), and 3-ethynylbenzaldehyde (1.0 g, 7.69 mmol) were successively added to a degassed solution of 1,3,5-tribromobenzene (1.20 g, 3.85 mmol) in dry Et_3N (8 mL) and THF (3 mL). The reaction mixture was heated to reflux under N_2 for 10 h. The solvents were removed under reduced pressure. The residue was taken up with CH_2Cl_2 and washed with water. The organic layer was dried over MgSO_4 . After the solvent was removed, the residue was purified by column chromatography (silica gel, $\text{CH}_2\text{Cl}_2/\text{petroleum ether}$, 3:1 v/v). Yield: 0.95 g (60%) of a yellow solid. $^1\text{H NMR}$ (CDCl_3 , 400 MHz, TMS): $\delta = 10.03$ (s, 2H), 8.03 (s, 2H), 7.88 (d, $J = 7.6$ Hz, 2H), 7.76 (d, $J = 8.0$ Hz, 2H), 7.66 (d, $J = 8.8$ Hz, 3H), 7.54 ppm (t, 2H, $J = 7.6$ Hz); TOF-MS (EI) $^+$: m/z : calcd for $\text{C}_{24}\text{H}_{13}\text{Br}_2\text{O}_2$: 412.0099 $[\text{M}+\text{H}]^+$; found: 412.0111.

Compound 23: [$\text{Pd}(\text{PPh}_3)_4$] (60.0 mg, 0.05 mmol), CuI (10.0 mg, 0.05 mmol), and **17** (0.48 g, 1.71 mmol) were successively added to a degassed solution of **22** (0.85 g, 2.1 mmol) in dry Et_3N (5 mL) and THF (3 mL). The reaction mixture was heated to reflux under N_2 for 8 h. The solvents were removed. The residue was washed with water and CH_2Cl_2 . The organic layer was dried over MgSO_4 . After the solvent was removed under reduced pressure, the residue was purified by column chromatography (silica gel, $\text{CH}_2\text{Cl}_2/\text{petroleum ether}$, 3:1 v/v). Yield: 0.60 g (60%) of a yellow oil. $^1\text{H NMR}$ (CDCl_3 , 400 MHz, TMS): $\delta = 10.01$ (s, 2H), 8.02 (s, 2H), 7.84 (d, $J = 7.6$ Hz, 2H), 7.75 (d, $J = 7.6$ Hz, 2H), 7.63 (s, 3H), 7.50 (t, $J = 7.6$ Hz, 2H), 7.29 (d, $J = 8.4$ Hz, 1H), 7.25 (s, 1H), 7.10–7.17 (m, 2H), 6.91 (t, $J = 7.2$ Hz, 1H), 6.84 (d, $J = 8.4$ Hz, 1H), 6.78 (d, $J = 8.4$ Hz, 1H), 3.82 (t, $J = 7.2$ Hz, 2H), 1.74–1.81 (m, 2H), 1.43–1.48 (m, 2H), 0.93 ppm (t, $J = 7.6$ Hz, 3H); APCI-MS: m/z : calcd for $\text{C}_{42}\text{H}_{29}\text{NO}_2\text{S}$: 612.19 $[\text{M}+\text{H}]^+$; found: 612.30.

Compound (S,S)-24: (S)-1-Phenylethanamine (0.17 g, 1.44 mmol) was added to a solution of **23** (0.40 g, 0.65 mmol) in dry THF (1 mL) and ethanol (5 mL). The reaction mixture was heated to reflux under nitrogen for 8 h. After the solution was cooled to RT, $\text{NaBH}_3(\text{CN})$ (0.21 g, 3.25 mmol) was added in several portions to the stirred solution, and the stirring was continued for 0.5 h. The resulting mixture was evaporated to dryness. The residue was taken up with CH_2Cl_2 and washed with water. The organic layer was dried over MgSO_4 . After removing the solvent, the residual was purified by column chromatography (silica gel, $\text{CH}_2\text{Cl}_2/\text{MeOH}$, 30:1 v/v). Yield: 0.40 g (75%) of a yellow oil. $^1\text{H NMR}$ (CDCl_3 , 400 MHz, TMS): $\delta = 7.61$ (s, 3H), 7.49 (s, 2H), 7.24–7.38 (m, 18H), 7.11–7.17 (m, 2H), 6.90 (t, $J = 8.0$ Hz, 1H), 6.85 (d, $J = 8.0$ Hz, 1H), 6.79 (d, $J = 8.0$ Hz, 1H), 3.80–3.87 (m, 4H), 3.58–3.68 (m, 4H), 1.75–1.82 (m, 2H), 1.39–1.51 (m, 8H), 0.93 ppm (t, $J = 8.0$ Hz, 3H); $^{13}\text{C NMR}$

(100 MHz, $\text{CDCl}_3/\text{CD}_3\text{OD}$): $\delta = 145.9$, 144.7, 141.5, 138.1, 134.0, 133.9, 131.4, 131.1, 130.6, 130.3, 130.0, 129.2, 128.6, 128.4, 127.9, 127.6, 127.5, 127.4, 125.0, 124.4, 124.2, 124.1, 122.3, 122.9, 122.7, 116.5, 115.7, 115.2, 94.6, 90.6, 90.3, 88.0, 87.8, 58.4, 57.4, 53.5, 47.4, 29.0, 20.2, 15.8, 13.9 ppm; TOF-MS (EI) $^+$: m/z : calcd for $\text{C}_{58}\text{H}_{51}\text{N}_3\text{S}$: 411.6980 $[\text{M}+2\text{H}]^{2+}$; found: 411.6967.

Sensor (S,S)-25: Compound (S,S)-24 (100.0 mg, 0.12 mmol), 2-(2-bromomethylphenyl)-1,3,2-dioxaborinane (68 mg, 0.26 mmol), and K_2CO_3 (99 g, 0.72 mmol) were mixed in dry MeCN (5 mL), then the mixture was heated to reflux for 10 h under N_2 . The reaction mixture was cooled to RT and diluted HCl was added. Then the mixture was stirred for a further 1 h. The solvent was removed under reduced pressure, and CH_2Cl_2 was added to take up the residue. The organic layer was washed with water and dried over anhydrous MgSO_4 . The solvent was removed under vacuum, and the residue was purified by column chromatography (silica gel, $\text{CH}_2\text{Cl}_2/\text{MeOH}$, 30:1 v/v). Yield: 42.0 mg (32%) of a light yellow powder. M.p. 204–205 °C; $[\alpha]_D^{25} = (-5.8 \pm 0.9)^\circ$ ($c = 0.15$ in CH_2Cl_2); $^1\text{H NMR}$ (CDCl_3 , 400 MHz): $\delta = 7.79$ (s, 2H), 7.62 (s, 3H), 7.25–7.43 (m, 22H), 7.11–7.19 (s, 6H), 6.91 (t, $J = 7.6$ Hz, 1H), 6.86 (d, $J = 8.4$ Hz, 1H), 6.81 (d, $J = 8.4$ Hz, 1H), 4.05–4.10 (m, 2H), 3.84–3.92 (m, 4H), 3.60–3.68 (m, 4H), 3.33–3.37 (m, 2H), 1.76–1.83 (m, 2H), 1.58 (d, $J = 7.2$ Hz, 6H), 1.42–1.51 (m, 2H), 0.93 ppm (t, $J = 7.2$ Hz, 3H); $^{13}\text{C NMR}$ (100 MHz, $\text{CDCl}_3/\text{CD}_3\text{OD}$): $\delta = 145.8$, 144.6, 141.4, 138.9, 137.9, 136.0, 133.9, 133.7, 132.8, 131.3, 131.0, 130.5, 130.2, 130.0, 129.9, 129.1, 128.5, 128.3, 127.8, 127.5, 127.4, 127.3, 124.9, 124.3, 124.1, 124.0, 122.8, 122.6, 116.4, 115.6, 115.1, 90.5, 90.2, 87.9, 87.6, 58.3, 57.3, 53.4, 47.3, 28.9, 20.1, 15.8, 13.8 ppm; TOF-MS (EI) $^+$: m/z : calcd for $\text{C}_{72}\text{H}_{65}\text{B}_2\text{N}_3\text{O}_4\text{S}$: 559.7676 $[\text{M}+2\text{MeOH}-2\text{H}_2\text{O}+2\text{H}]^{2+}$; found: 559.7643.

Compound (R,R)-24: This compound was synthesized by using a procedure similar to that of (S,S)-21. A yellow oil was obtained in a yield of 65%. $^1\text{H NMR}$ (CDCl_3 , 400 MHz, TMS): $\delta = 7.59$ (s, 3H), 7.50 (s, 2H), 7.35–7.42 (m, 9H), 7.26–7.33 (m, 9H), 7.11–7.17 (m, 2H), 6.91 (t, $J = 8.0$ Hz, 1H), 6.85 (d, $J = 8.0$ Hz, 1H), 6.80 (d, $J = 8.4$ Hz, 1H), 3.84–3.87 (m, 4H), 3.59–3.71 (m, 4H), 1.76–1.83 (m, 2H), 1.40–1.51 (m, 8H), 0.93 ppm (t, $J = 8.0$ Hz, 3H); $^{13}\text{C NMR}$ (100 MHz, $\text{CDCl}_3/\text{CD}_3\text{OD}$): $\delta = 145.8$, 144.6, 141.4, 138.8, 137.9, 136.1, 133.9, 133.8, 132.8, 131.0, 130.6, 130.3, 130.1, 129.9, 129.1, 128.6, 128.3, 127.8, 127.5, 127.4, 127.3, 124.9, 124.3, 124.1, 124.0, 122.9, 122.7, 116.4, 115.6, 115.2, 90.5, 90.2, 87.9, 87.7, 58.3, 57.3, 53.5, 53.4, 47.3, 31.0, 28.9, 20.2, 15.8, 13.9 ppm; TOF-MS (EI) $^+$: m/z : calcd for $\text{C}_{58}\text{H}_{51}\text{N}_3\text{S}$: 411.6980 $[\text{M}+2\text{H}]^{2+}$; found: 411.6987.

Sensor (R,R)-25: This compound was synthesized by using a procedure similar to that of (S,S)-25. A light-yellow powder was obtained in a yield of 30%. M.p. 204–205 °C; $[\alpha]_D^{25} = (-6.3 \pm 0.8)^\circ$ ($c = 0.15$ in CH_2Cl_2); $^1\text{H NMR}$ (CDCl_3 , 400 MHz, TMS): $\delta = 7.81$ (d, $J = 8.0$ Hz, 2H), 7.62 (s, 3H), 7.25–7.43 (m, 22H), 7.11–7.19 (m, 6H), 6.91 (t, $J = 7.6$ Hz, 1H), 6.86 (d, $J = 8.0$ Hz, 1H), 6.81 (d, $J = 8.8$ Hz, 1H), 4.05–4.10 (m, 2H), 3.84–3.93 (m, 4H), 3.60–3.67 (m, 4H), 3.33–3.36 (m, 2H), 1.76–1.83 (m, 2H), 1.58 (d, $J = 7.2$ Hz, 6H), 1.42–1.51 (m, 2H), 0.93 ppm (t, $J = 7.2$ Hz, 3H); $^{13}\text{C NMR}$ (100 MHz, $\text{CDCl}_3/\text{CD}_3\text{OD}$): $\delta = 145.8$, 144.6, 141.4, 138.8, 137.9, 136.1, 134.9, 133.9, 133.8, 132.8, 131.4, 131.0, 130.6, 130.3, 130.1, 129.9, 129.2, 128.6, 128.3, 127.8, 127.5, 127.4, 127.3, 124.9, 124.3, 124.0, 122.9, 122.7, 116.4, 115.6, 115.2, 90.5, 90.2, 87.9, 87.7, 58.3, 57.3, 53.5, 53.4, 47.3, 31.0, 28.9, 20.2, 15.8, 13.8 ppm; TOF-MS (EI) $^+$: m/z : calcd for $\text{C}_{72}\text{H}_{65}\text{B}_2\text{N}_3\text{O}_4\text{S}$: 559.7676 $[\text{M}+2\text{MeOH}-2\text{H}_2\text{O}+2\text{H}]^{2+}$; found: 559.7665.

Acknowledgements

We thank the NSFC (20972024 and 21073028), Fundamental Research Funds for the Central Universities (DUT10ZD212), the Royal Society (UK) and NSFC (China) (China/UK Cost-Share Program, 21011130154), the Ministry of Education (SRFDP-200801410004 and NCET-08-0077), the Education Department of Liaoning Province (2009T015), the State Key Laboratory of Fine Chemicals (KF0802), and Dalian University of Technology for financial support. We also thank the Catalysis and Sensing for our Environment (CASE) consortium for networking opportuni-

ties. T.D.J. would also like to thank Dalian University of Technology for the award of a HaiTian Scholarship.

- [1] T. D. James, *Top. Curr. Chem.* **2007**, *277*, 107–152.
- [2] H. Liu, X. Hou, L. Pu, *Angew. Chem.* **2009**, *121*, 388–391; *Angew. Chem. Int. Ed.* **2009**, *48*, 382–385.
- [3] N. Fujita, S. Shinkai, T. D. James, *Chem. Asian J.* **2008**, *3*, 1076–1091.
- [4] B. T. Nguyen, E. V. Anslyn, *Coord. Chem. Rev.* **2006**, *250*, 3118–3127.
- [5] A. T. Wright, E. V. Anslyn, *Chem. Soc. Rev.* **2006**, *35*, 14–28.
- [6] L. Pu, *Chem. Rev.* **1998**, *98*, 2405–2494.
- [7] L. Pu, *Chem. Rev.* **2004**, *104*, 1687–1716.
- [8] T. Gunnlaugsson, M. Glynn, G. M. Tocci, P. E. Kruger, F. M. Pfeffer, *Coord. Chem. Rev.* **2006**, *250*, 3094–3117.
- [9] G. Mirri, S. D. Bull, P. N. Horton, T. D. James, L. Male, J. H. R. Tucker, *J. Am. Chem. Soc.* **2010**, *132*, 8903–8905.
- [10] G. V. Oshovsky, D. N. Reinhoudt, W. Verboom, *Angew. Chem.* **2007**, *119*, 2418–2445; *Angew. Chem. Int. Ed.* **2007**, *46*, 2366–2393.
- [11] J. J. Lavigne, E. V. Anslyn, *Angew. Chem.* **1999**, *111*, 3903–3906; *Angew. Chem. Int. Ed.* **1999**, *38*, 3666–3669.
- [12] L. Zhu, Z. Zhong, E. V. Anslyn, *J. Am. Chem. Soc.* **2005**, *127*, 4260–4269.
- [13] a) L. Zhu, S. H. Shabbir, M. Gray, V. M. Lynch, S. Sorey, E. V. Anslyn, *J. Am. Chem. Soc.* **2006**, *128*, 1222–1232; b) B. E. Collins, S. Sorey, A. E. Hargrove, S. H. Shabbir, V. M. Lynch, E. V. Anslyn, *J. Org. Chem.* **2009**, *74*, 4055–4060.
- [14] S. Jin, J. Wang, M. Li, B. Wang, *Chem. Eur. J.* **2008**, *14*, 2795–2804.
- [15] C. J. Musto, S. H. Lim, K. S. Suslick, *Anal. Chem.* **2009**, *81*, 6526–6533.
- [16] A. Nonaka, S. Horie, T. D. James, Y. Kubo, *Org. Biomol. Chem.* **2008**, *6*, 3621–3625.
- [17] K. M. K. Swamy, S. K. Ko, S. K. Kwon, H. N. Lee, C. Mao, J. M. Kim, K. H. Lee, J. Kim, I. Shin, J. Yoon, *Chem. Commun.* **2008**, 5915–5917.
- [18] W. M. J. Ma, M. P. P. Morais, F. D. Hooge, J. M. H. Elsen, J. P. L. Cox, T. D. James, J. S. Fossey, *Chem. Commun.* **2009**, 532–534.
- [19] L. Zhang, J. A. Kerszulis, R. J. Clark, T. Ye, L. Zhu, *Chem. Commun.* **2009**, 2151–2153.
- [20] S. M. Levonis, M. J. Kiefel, T. A. Houston, *Chem. Commun.* **2009**, 2278–2280.
- [21] D. A. Köse, B. Zümreoglu-Karan, *New J. Chem.* **2009**, *33*, 1874–1881.
- [22] G. Heinrichs, M. Schellentraeger, S. Kubik, *Eur. J. Org. Chem.* **2006**, 4177–4186.
- [23] M. Dowlut, D. G. Hall, *J. Am. Chem. Soc.* **2006**, *128*, 4226–4227.
- [24] S. H. Shabbir, L. A. Joyce, G. M. Da Cruz, V. M. Lynch, S. Sorey, E. V. Anslyn, *J. Am. Chem. Soc.* **2009**, *131*, 13125–13131.
- [25] a) J. Zhao, T. M. Fyles, T. D. James, *Angew. Chem.* **2004**, *116*, 3543–3546; *Angew. Chem. Int. Ed.* **2004**, *43*, 3461–3464; b) J. Zhao, M. G. Davidson, M. F. Mahon, G. Kociok-Kohn, T. D. James, *J. Am. Chem. Soc.* **2004**, *126*, 16179–16186; c) J. Zhao, T. D. James, *J. Mater. Chem.* **2005**, *15*, 2896–2901; d) J. Zhao, T. D. James, *Chem. Commun.* **2005**, 1889–1891; e) L. Chi, J. Zhao, T. D. James, *J. Org. Chem.* **2008**, *73*, 4684–4687; f) F. Han, L. Chi, X. Liang, S. Ji, S. Liu, F. Zhou, Y. Wu, K. Han, J. Zhao, T. D. James, *J. Org. Chem.* **2009**, *74*, 1333–1336; g) X. Zhang, L. Chi, S. Ji, Y. Wu, P. Song, K. Han, H. Guo, T. D. James, J. Zhao, *J. Am. Chem. Soc.* **2009**, *131*, 17452–17463; h) X. Zhang, Y. Wu, S. Ji, H. Guo, P. Song, K. Han, W. Wu, W. Wu, T. D. James, J. Zhao, *J. Org. Chem.* **2010**, *75*, 2578–2588.
- [26] T. D. James, K. R. A. S. Sandanayake, S. Shinkai, *Nature* **1995**, *374*, 345–347.
- [27] Z. Li, J. Lin, M. Sabat, M. Hyacinth, L. Pu, *J. Org. Chem.* **2007**, *72*, 4905–4916.
- [28] Q. Wang, X. Chen, L. Tao, L. Wang, D. Xiao, X. Yu, L. Pu, *J. Org. Chem.* **2007**, *72*, 97–101.
- [29] L. Zhu, E. V. Anslyn, *J. Am. Chem. Soc.* **2004**, *126*, 3676–3677.
- [30] G. Ajayakumar, K. Sreenath, K. R. Gopidas, *Dalton Trans.* **2009**, 1180–1186.
- [31] S. Chakraborty, T. J. Wadas, H. Hester, R. Schmehl, R. Eisenberg, *Inorg. Chem.* **2005**, *44*, 6865–6878.
- [32] T. D. James, H. Shinmori, S. Shinkai, *Chem. Commun.* **1997**, 71–72.
- [33] a) J. D. Larkin, J. S. Fossey, T. D. James, B. R. Brooks, C. W. Bock, *J. Phys. Chem. A* **2010**, *114*, 12531–12539; b) Y. Liu, J. Feng, A. Ren, *J. Phys. Chem. A* **2008**, *112*, 3157–3164.
- [34] O. A. Borg, S. S. M. C. Godinho, M. J. Lundqvist, S. Lunell, P. Persson, *J. Phys. Chem. A* **2008**, *112*, 4470–4476.
- [35] G. Zhao, J. Liu, L. Zhou, K. Han, *J. Phys. Chem. A* **2007**, *111*, 8940–8945.
- [36] S. Ji, J. Yang, Q. Yang, S. Liu, M. Chen, J. Zhao, *J. Org. Chem.* **2009**, *74*, 4855–4865.
- [37] S. Ji, H. Guo, X. Yuan, X. Li, H. Ding, P. Gao, C. Zhao, W. Wu, W. Wu, J. Zhao, *Org. Lett.* **2010**, *12*, 2876–2879.
- [38] B. Valeur, *Molecular Fluorescence: Principles and Applications*, Wiley-VCH, Weinheim, **2002**.
- [39] W. Yang, H. Fan, X. Gao, S. Gao, V. V. R. Karnati, W. Ni, W. B. Hooks, J. Carson, B. Weston, B. Wang, *Chem. Biol.* **2004**, *11*, 439–448.
- [40] a) A. E. Hargrove, R. N. Reyes, I. Riddington, E. V. Anslyn, J. L. Sessler, *Org. Lett.* **2010**, *12*, 4804–4807; b) S. Jin, C. Zhu, Y. Cheng, M. Li, B. Wang, *Bioorg. Med. Chem.* **2010**, *18*, 1449–1455.
- [41] C. Xue, F. Cai, H. Liu, *Chem. Eur. J.* **2008**, *14*, 1648–1653.
- [42] Gaussian 09, Revision A.1, M. J. Frisch, G. W. Trucks, H. B. Schlegel, G. E. Scuseria, M. A. Robb, J. R. Cheeseman, G. Scalmani, V. Barone, B. Mennucci, G. A. Petersson, H. Nakatsuji, M. Caricato, X. Li, H. P. Hratchian, A. F. Izmaylov, J. Bloino, G. Zheng, J. L. Sonnenberg, M. Hada, M. Ehara, K. Toyota, R. Fukuda, J. Hasegawa, M. Ishida, T. Nakajima, Y. Honda, O. Kitao, H. Nakai, T. Vreven, J. A. Montgomery, Jr., J. E. Peralta, F. Ogliaro, M. Bearpark, J. J. Heyd, E. Brothers, K. N. Kudin, V. N. Staroverov, R. Kobayashi, J. Normand, K. Raghavachari, A. Rendell, J. C. Burant, S. S. Iyengar, J. Tomasi, M. Cossi, N. Rega, J. M. Millam, M. Klene, J. E. Knox, J. B. Cross, V. Bakken, C. Adamo, J. Jaramillo, R. Gomperts, R. E. Stratmann, O. Yazyev, A. J. Austin, R. Cammi, C. Pomelli, J. W. Ochterski, R. L. Martin, K. Morokuma, V. G. Zakrzewski, G. A. Voth, P. Salvador, J. J. Dannenberg, S. Dapprich, A. D. Daniels, Ö. Farkas, J. B. Foresman, J. V. Ortiz, J. Cioslowski, D. J. Fox, Gaussian, Inc., Wallingford CT, **2009**.

Received: January 5, 2011
Published online: May 19, 2011